



09-21-00

A

mom

Please type a plus sign (+) inside this box → 

PTO/SB/05 (4/98)

Approved for use through 09/30/00. OMB 0651-0032

Patent and Trademark Office: U.S. DEPARTMENT OF COMMERCE

Under the Paperwork Reduction Act of 1995, no persons are required to respond to a collection of information unless it displays a valid OMB control number.

# UTILITY PATENT APPLICATION TRANSMITTAL

(Only for new nonprovisional applications under 37 CFR 1.53(b))

Atty. Docket No. X-501-1P US

First Inventor or Appl. Identifier

Title Tunable Narrow-Band Filter Including Sigma-Delta Modulator

Express Mail Label No. EL539651173US

PRE

**APPLICATION ELEMENTS**

See MPEP chapter 600 concerning utility patent application contents.

- |  |  |
|--|--|
| <p>1. <input checked="" type="checkbox"/> *Fee Transmittal Form (e.g., PTO/SB/17)<br/>(Submit an original, and a duplicate for fee processing)</p> <p>2. <input checked="" type="checkbox"/> Specification [Total Pages (preferred arrangement set forth below)]<br/>           - Descriptive title of the Invention<br/>           - Cross References to Related Applications<br/>           - Statement Regarding Fed sponsored R &amp; D<br/>           - Reference to Microfiche Appendix<br/>           - Background of the Invention<br/>           - Brief Summary of the Invention<br/>           - Brief Description of the Drawings (if filed)<br/>           - Detailed Description<br/>           - Claim(s)<br/>           - Abstract of the Disclosure</p> <p>3. <input checked="" type="checkbox"/> Drawing(s) (35 USC 113) [Total Sheets 20]</p> <p>4. Oath or Declaration [Total Pages 2]</p> <p>a. <input type="checkbox"/> Newly executed (original or copy)<br/>           b. <input type="checkbox"/> Copy from a prior application (37 CFR § 1.63(d))<br/>           (for continuation/divisional with Box 16 completed)</p> | <p>36</p> <p>5. <input type="checkbox"/> Microfiche Computer Program (Appendix)<br/>           6. <input type="checkbox"/> Nucleotide and/or Amino Acid Sequence Submission<br/>           (if applicable, all necessary)<br/>           a. <input type="checkbox"/> Computer Readable Copy<br/>           b. <input type="checkbox"/> Paper Copy (identical to computer copy)<br/>           c. <input type="checkbox"/> Statement verifying identity of above copies</p> |
|--|--|

**ACCOMPANYING APPLICATION PARTS**

7.  Assignment Papers (cover sheet & document(s))  
 8.  37 CFR §3.73(b) Statement  Power of Attorney  
 (when there is an assignee)  
 9.  English Translation Document (if applicable)  
 10.  Information Disclosure Statement (IDS)/PTO-1449  Copies of IDS Citations  
 11.  Preliminary Amendment  
 12.  Return Receipt Postcard (MPEP 503)  
 (Should be specifically itemized)  
 \*Small Entity  Statement filed in prior application.  
 13.  Statement(s)  Status still proper and desired  
 (PTO/SB/09-12)  
 14.  Certified Copy of Priority Document(s)  
 (if foreign priority is claimed)  
 15.  Other: .....

**NOTE FOR ITEMS 1 & 13.** IN ORDER TO BE ENTITLED TO PAY SMALL ENTITY FEES, A SMALL ENTITY STATEMENT IS REQUIRED (37 C.F.R. § 127), EXCEPT IF ONE FILED IN A PRIOR APPLICATION IS RELIED UPON (37 C.F.R. § 128)

16. If a **CONTINUING APPLICATION**, check appropriate box and supply the requisite information below and in a preliminary amendment:

Continuation  Divisional  Continuation-in-part (CIP) of prior application No: 09/394,123

Prior application information: Examiner \_\_\_\_\_ Not Yet Known Group / Art Unit: 2734

**For CONTINUATION or DIVISIONAL APPS only:** The entire disclosure of the prior application, from which an oath or declaration is supplied under Box 4b, is considered a part of the disclosure of the accompanying continuation or divisional application and is hereby incorporated by reference. The incorporation can only be relied upon when a portion has been inadvertently omitted from the submitted application parts.

**18. CORRESPONDENCE ADDRESS**

Customer Number or Bar Code Label **24309** or  Correspondence address below  
(Insert Customer No. or Attach bar code label here)

Name	<b>Attn: Edel M. Young</b>				
Address					
City		State		Zip Code	
Country		Telephone	408-879-4969	Fax	408-377-6137

Name (Print/Type)	Edel M. Young	Registration No. (Attorney/Agent)	32,451
Signature	<i>Edel M. Young</i>	Date	September 20, 2000

Burden Hour Statement: This form is estimated to take 0.2 hours to complete. Time will vary depending upon the needs of the individual case. Any comments on the amount of time you are required to complete this form should be sent to the Chief Information Officer, Patent and Trademark Office, Washington, DC 20231. DO NOT SEND FEES OR COMPLETED FORMS TO THIS ADDRESS. SEND TO: Assistant Commissioner for Patents, Box Patent Application, Washington, DC 20231.

Under the Paperwork Reduction Act of 1995, no persons are required to respond to a collection of information unless it displays a valid OMB control number.

# FEE TRANSMITTAL for FY 2000

Patent fees are subject to annual revision

Small Entity payments must be supported by a small entity statement, otherwise large entity fees must be paid. See Forms PTO/SB/09-12. See 37 C.F.R. §§ 1.27 and 1.28.

TOTAL AMOUNT OF PAYMENT (\$ 690.00)

## Complete if Known

Application Number	Not Yet Known
Filing Date	September 20, 2000
First Named Inventor	Christopher H. Dick
Examiner Name	Not Yet Known
Group / Art Unit	Not Yet Known

Attorney Docket No. X-501-1P US

## METHOD OF PAYMENT (check one)

1.  The Commissioner is hereby authorized to charge indicated fees and credit any over payments to:

Deposit Account Number 24-0040

Deposit Account Name XILINX, INC.

 Charge the Issue Fee Required Under 37 CFR §§ 1.16 and 1.172.  Payment Enclosed: Check     Money Order     Other

## FEE CALCULATION

## 1. BASIC FILING FEE

Large Entity			
Fee Paid	Fee	Fee Description	Fee
Code	(\$)		\$690
101	760	Utility filing fee	
106	330	Design filing fee	
107	540	Plant filing fee	
108	760	Reissue filing fee	
114	150	Provisional filing fee	
SUBTOTAL (1)		(\$)	690.00

## 2. EXTRA CLAIM FEES

	Extra	Fee from below	Fee Paid
Total Claims	1	-20** = -19	X = \$0
Indep. Claims	1	- 3** = -2	X = \$0
Multiple Dependent		X =	

\*\*or number previously paid, if greater, For Reissues, see below

Large Entity		
Fee Code	Fee (\$)	Fee Description
103	18	Claims in excess of 20
102	78	Independent claims in excess of 3
104	260	Multiple dependent claim, if not paid
109	78	**Reissue independent claims over original patent
110	18	**Reissue claims in excess of 20 and over original patent
SUBTOTAL (2)		(\$ 0.00)

## FEE CALCULATION (continued)

## 3. ADDITIONAL FEES

Large Entity Fee Code	Fee (\$)	Fee Description	Fee Paid
105	130	Surcharge - late filing fee or oath	
127	50	Surcharge - late provisional filing fee or cover sheet.	
147	2,520	For filing a request for reexamination	
112	920*	Requesting publication of SIR prior to Examiner action	
113	1,840*	Requesting publication of SIR after Examiner action	
115	110	Extension for reply within first month	
116	380	Extension for reply within second month	
117	870	Extension for reply within third month	
118	1,360	Extension for reply within fourth month	
128	1,850	Extension for reply within fifth month	
119	300	Notice of Appeal	
120	300	Filing a brief in support of an appeal	
121	260	Request for oral hearing	
138	1,510	Petition to institute a public use proceeding	
140	110	Petition to revive - unavoidable	
141	1,210	Petition to revive - unintentional	
142	1,210	Utility issue fee (or reissue)	
122	130	Petitions to the Commissioner	
123	50	Petitions related to provisional applications	
126	240	Submission of Information Disclosure Stmt	
581	40	Recording each patent assignment per property (times number of properties)	
146	690	Filing a submission after final rejection (37 CFR 1.129(a))	
149	690	For each additional invention to be examined (37 CFR 1.129(b))	
Other fee (specify) _____			
Other fee (specify) _____			

\*Reduced by Basic Filing Fee Paid SUBTOTAL (3) (\$)

## SUBMITTED BY

Complete (if applicable)

Name (Print/Type)	Edel M. Young	Registration No. (Attorney/Agent)	32,451	Telephone	408-879-4969
Signature	Edel M. Young			Date	09-20-2000

Burden Hour Statement: This form is estimated to take 0.2 hours to complete. Time will vary depending upon the needs of the individual case. Any comments on the amount of time you are required to complete this form should be sent to the Chief Information Officer, Patent and Trademark Office, Washington, DC 20231. DO NOT SEND FEES OR COMPLETED FORMS TO THIS ADDRESS. SEND TO: Assistant Commissioner for Patents, Washington, DC 20231.

1                   TUNABLE NARROW-BAND FILTER INCLUDING  
2                   SIGMA-DELTA MODULATOR

3  
4                   Christopher H. Dick  
5                   Frederic J. Harris

6  
7 CROSS-REFERENCE TO RELATED APPLICATION

8                   This is a continuation-in-part of U.S. Patent Application  
9                   Serial No. 09/394,123 filed 9/10/1999 entitled "Narrow Band  
10                  Filter Including Sigma-Delta Modulator Implemented in a  
11                  Programmable Logic Device", incorporated herein by reference.

12  
13 INTRODUCTION

14                  While  $\Sigma\Delta M$  techniques are applied widely in analog  
15                  conversion sub-systems, both analog-to-digital (ADC) and  
16                  digital-to-analog (DAC) converters, these methods have  
17                  enjoyed much less exposure in the broader application  
18                  domain, where flexible and configurable solutions,  
19                  traditionally supplied via a software DSP (soft-DSP), are  
20                  required. And this limited level of exposure is easy to  
21                  understand. Most, if not all, of the efficiencies and  
22                  optimizations afforded by  $\Sigma\Delta M$  are hardware oriented and so  
23                  cannot be capitalized on in the fixed precision pre-defined  
24                  datapath found in a soft-DSP processor. This limitation, of  
25                  course, does not exist in a field programmable gate array  
26                  (FPGA) DSP solution. With FPGAs the designer has complete  
27                  control of the silicon to implement any desired datapath and  
28                  employ optimal word precisions in the system with the  
29                  objective of producing a design that satisfies the  
30                  specifications in the most economically sensitive manner.

EL539651173US

1        While implementation of a digital  $\Sigma\Delta$  ASIC (application-  
2 specific integrated circuit) is of course possible, economic  
3 constraints make the implementation of such a building block  
4 that would provide the flexibility, and be generic enough to  
5 cover a broad market cross-section, impractical. FPGA-based  
6 hardware provides a solution to this problem. FPGAs are off-  
7 the-shelf commodity items that provide a silicon feature set  
8 ideal for constructing high-performance DSP systems. These  
9 devices maintain the flexibility of software-based  
10 solutions, while providing levels of performance that match,  
11 and often exceed ASIC solutions.

12      There is a rich and expanding body of literature  
13 devoted to the efficient and effective implementation of  
14 digital signal processors using FPGA based hardware. More  
15 often than not, the most successful of these techniques  
16 involves a paradigm shift away from the methods that provide  
17 good solutions in software programmable DSP systems.

18      This paper reports on the rich set of design  
19 opportunities that are available to the signal processing  
20 system designer through innovative combinations of  $\Sigma\Delta M$   
21 techniques and FPGA signal processing hardware. The  
22 applications considered include narrow-band filters, both  
23 single-rate and multi-rate, DC canceler, and  $\Sigma\Delta M$  hybrid  
24 digital-analog control loops for simplifying carrier  
25 recovery, timing recovery, and AGC (automatic gain control)  
26 loops in a digital communication receiver.

27      This application is organized as follows: section 2  
28 presents a brief overview of FPGA architecture. In section 3  
29 a simple single-loop base-band  $\Sigma\Delta$  modulator is introduced.  
30 The structure is extended to a normal architecture that

1 permits center frequency tuning, as well as a method for  
2 working with the system degrees of freedom to trade-off  
3 modulator bandwidth with dynamic range. The tunable  $\Sigma\Delta M$  is  
4 then utilized for implementing area efficient FPGA FIR  
5 filters. The process for computing the modulator  
6 coefficients for low pass, bandpass, and high pass designs  
7 is described. In section 4, a new  $\Sigma\Delta M$  architecture is  
8 described that provides a very simple method for tuning  
9 using only a single coefficient. In any fixed-point data  
10 path, careful consideration must be given to the DC aspects  
11 of the design. For example, the introduction of a DC  
12 complement to two-step altercation between the stages of a  
13 multi-stage, multi-rate filter can be problematic, causing  
14 arithmetic saturation or increasing the bit error rates in  
15 additional receiver. Section 5 describes a unique  $\Sigma\Delta M$   
16 approach to building a DC canceler. In section 6,  $\Sigma\Delta M$   
17 methods are described for simplifying the implementation of  
18 hybrid digital-analog control loops in a system such as a  
19 software-defined radio. In section 7 some comments on the  
20 industrial implications of the techniques considered in the  
21 application are presented. Finally, some conclusions are  
22 drawn in section 8.

23 Semiconductor vendors, such as Xilinx, Altera, Atmel,  
24 and AT&T, provide a range of FPGAs. The architectural  
25 approaches are as diverse as there are manufacturers, but  
26 some generalizations can be made. Most of the devices are  
27 basically organized as an array of logic elements and  
28 programmable routing resources used to provide the  
29 connectivity between the logic elements, FPGA I/O pins and  
30 other resources, such as on-chip memory. The structure and

1 complexity of the logic elements, as well as the  
2 organization and functionality supported by the  
3 interconnection hierarchy, distinguish the devices. Other  
4 device features, such as block memory and delay locked loop  
5 technology, are also significant factors that influence the  
6 complexity and performance of an algorithm that is  
7 implemented using FPGAs.

8 A logic element usually consists of one or more RAM  
9 (random access memory) n-input look-up tables, where n is  
10 between three and 6, in one to several flip-flops. There may  
11 also be additional hardware support in each element to  
12 enable high-speed arithmetic operations. This generic FPGA  
13 architecture is shown in Figure 1. Also illustrated in the  
14 Figure (as wide lines) are several connections between logic  
15 elements and the device input/output (I/O) ports.

16 Application-specific circuitry is supported in the device by  
17 downloading a bit stream into SRAM (static random access  
18 memory) based configuration memory. This personalization  
19 database defines the functionality of the logic elements, as  
20 well as the internal routing. Different applications are  
21 supported on the same FPGA hardware platform by configuring  
22 the FPGA(s) with appropriate bit streams. As a specific  
23 example, consider the Xilinx Virtex™ series of FPGAs. The  
24 logic elements, called slices, essentially consist of four-input  
25 look-up tables (LUTs), to flip-flops, several  
26 multiplexors and some additional silicon support that allows  
27 the efficient implementation of carry-chains for building  
28 high-speed multipliers, subtracters, and shift registers. Two  
29 slices form a configurable logic block (CLB) as shown in  
30 Figure 2. The CLB is the basic tile used to build the  
31 logic matrix. Some FPGAs, like the Xilinx Virtex families,

1 supplying on-chip block RAM. Figure 3 shows the CLB matrix  
2 that defines a Virtex FPGA. Current generation Virtex  
3 silicon provides a family of devices offering 768 to 12,288  
4 logic slices, and from 8 to 32 variable form factor block  
5 memories.

6 Xilinx XC4000 and Virtex devices also allow the  
7 designer to use the logic element LUTs as memory-either ROM  
8 or RAM. Constructing memory with this distributed memory  
9 approach can yield access bandwidths in many pps at GB per  
10 second range.

11 Typical clock frequencies for current generation  
12 devices are in the multiple tens of megahertz (100 to  
13 200) range.

14 In contrast to the logic slice architecture employed in  
15 Xilinx Virtex devices, a logic block architecture employed  
16 in the Atmel AT40K FPGA is shown in Figure 4. Like the  
17 Xilinx device, combinational logic is realized using look-up  
18 tables. In this case, to three-input LUTs and a single flip-  
19 flop are available in each logic cell. The pass gates in a  
20 cell form part of the signal routing network and are used  
21 for connecting signals to the multiple horizontal and  
22 vertical bus plains. In addition to the orthogonal routing  
23 resources, indicated as N, S, E and W in Figure 4, a  
24 diagonal group of interconnects (NW, NE, SE, and SW),  
25 associated with each cell x output, are available to provide  
26 efficient connections to neighboring cell's x bus inputs.

27 The objective of the FPGA/DSP architect is to formulate  
28 algorithmic solutions for applications that best utilize  
29 FPGA resources to achieve the required functionality. This  
30 is a three-dimensional optimization problem in power,  
31 complexity, and bandwidth. The remainder of this application

1 describes some novel FPGA solutions to several signal  
2 processing problems. The results are important in industrial  
3 context because they enable either smaller, and hence more  
4 economic, solutions to important problems, or allow more  
5 arithmetic compute power to be realized with a given area of  
6 silicon.

7

8

9  $\Sigma\Delta$  MODULATORS, FIR FILTERS AND FPGAS

10        $\Sigma\Delta$ -based DSP is employed to generate FPGA hardware  
11 implementations of narrow-band filters, a DC canceller, and  
12 hybrid digital-analog control loops for a software-defined  
13 radio architecture.

14

15       This section describes a method employing sigma-delta  
16 modulation ( $\Sigma\Delta$ ) techniques for implementing area efficient  
17 finite impulse response (FIR) filters using FPGA hardware.  
18 Before treating the FPGA filter design, a brief review of  $\Sigma\Delta$   
19 modulation encoding is presented.

20

21  $\Sigma\Delta$  Modulation

22       Sigma-Delta modulation is a source coding technique  
23 most prominently employed in analog-to-digital and digital-  
24 to-analog converters. In this context, hybrid analog and  
25 digital circuits are used in the realization. Figure 5 shows  
26 a single-loop  $\Sigma\Delta$  modulator. Provided the input signal is  
27 busy enough, the linearized discrete time model of Figure 6  
28 can be used to illustrate the principle. In Figure 6, the 1-  
29 bit quantizer is modeled by an additive white noise source

1 with variance  $\sigma_e^2 = \Delta^2/12$ , where  $\Delta$  represents the quantization  
2 interval. The z-transform  
3 of the system is

4  
5 Equations 1 and 2:

$$\begin{aligned} Y(z) &= \frac{H(z)}{1+H(z)} X(z) + \frac{1}{1+H(z)} Q(z) \\ &= H_s(z)X(z) + H_n(z)Q(z) \end{aligned}$$

6 where

7  
8 Equation 3:

$$H(z) = \frac{1}{z-1}$$

9  
10 which is the transfer function of delay and an ideal  
11 integrator, and  $H_s(z)$  and  $H_n(z)$  are the signal and noise  
12 transfer functions (NTF) respectively. In a good  $\Sigma\Delta$   
13 modulator,  $H_n(\omega)$  will have a flat frequency response in the  
14 interval  $|f| \leq B$ . In contrast,  $H_n(\omega)$  will have a high  
15 attenuation in the frequency band  $|f| \leq B$  and a "don't care"  
16 region in the interval  $B < |f| < f_s/2$ . For the single loop  $\Sigma\Delta$   
17 in Figure 6,  $H_s(z) = z^{-1}$  and  $H_n(z) = 1-z^{-1}$ . Thus the input  
18 signal is not distorted in any way by the network and simply  
19 experiences a pure delay from input to output. The  
20 performance of the system is determined by the noise  
21 transfer function  $H_n(z)$ , which is given by

22  
23 Equation 4:

$$|H_n(f)| = 4 \left| \sin \frac{\pi f}{f_s} \right|$$

1  
2 and is shown in Figure 7. The in-band quantization noise  
3 variance is  
4  
5 Equation 5:

$$\sigma_n^2 = \int_{-B}^{+B} |H_n(f)|^2 S_q(f) df$$

6  
7 where  $S_q(f) = \sigma_q^2 / f_s$  is the power spectral density of the  
8 quantization noise. Observe that for a non-shaped noise (or  
9 white) spectrum, increasing the sampling rate by a factor of  
10 2, while keeping the bandwidth B fixed, reduces the  
11 quantization noise by 3 dB. For a first order  $\Sigma\Delta M$  it can be  
12 shown that

13  
14 Equation 6:

$$\sigma_n^2 \approx \frac{1}{3} \pi^2 \sigma_q^2 \left( \frac{2B}{f_s} \right)^3$$

15  
16 for  $f_s \gg 2B$ . Under these conditions doubling the sampling  
17 frequency reduces the noise power by 9 dB, of which 3 dB is  
18 due to the reduction in  $S_q(f)$  and a further 6 dB is due to  
19 the filter characteristic  $H_n(f)$ . The noise power is reduced  
20 by increasing the sampling rate to spread the quantization  
21 noise over a large bandwidth and then by shaping the power  
22 spectrum using an appropriate filter.

23

24 Reduced Complexity Filters Using  $\Sigma\Delta$  Modulation Techniques

1        $\Sigma\Delta$ M techniques can be employed for realizing area  
2 efficient narrowband filters in FPGAs. These filters are  
3 utilized in many applications. For example, narrow-band  
4 communication receivers, multi-channel RF surveillance  
5 systems and for solving some spectrum management problems.

6       A uniform quantizer operating at the Nyquist rate is  
7 the standard solution to the problem of representing data  
8 within a specified dynamic range. Each additional bit of  
9 resolution in the quantizer provides an increase in dynamic  
10 range of approximately 6dB. A signal with 60dB of dynamic  
11 range requires 10 bits, while 16 bits can represent data  
12 with a dynamic range of 96dB.

13      While the required dynamic range of a system fixes the  
14 number of bits required to represent the data, it also  
15 affects the expense of subsequent arithmetic operations, in  
16 particular multiplications. In any hardware implementation,  
17 and of course this includes FPGA based DSP processors, there  
18 are strong economic imperatives to minimize the number and  
19 complexity of the arithmetic components employed in the  
20 datapath. An embodiment of the invention employs noise-  
21 shaping techniques to reduce the precision of the input data  
22 samples to minimize the complexity of the multiply-  
23 accumulate (MAC) units in the filter. The net result is a  
24 reduction in the amount of FPGA logic resources required to  
25 realize the specified filter.

26      Consider the structure shown in Figure 8. Instead of  
27 applying the quantized data  $x(n)$  from the analog-to-digital  
28 converter directly to the filter, data  $x(n)$  is pre-processed  
29 by a  $\Sigma\Delta$  modulator. The re-quantized input samples  $\hat{x}(n)$  are  
30 represented using fewer bits per sample, so permitting the

1 subsequent filter  $H(z)$  to employ reduced precision  
2 multipliers in the mechanization. The filter coefficients  
3 are still kept to a high precision.

4       The  $\Sigma\Delta$  data re-quantizer is based on a single loop  
5 error feedback sigma-delta modulator shown in Figure 9. In  
6 this configuration, the difference between the quantizer  
7 input and output sample is a measure of the quantization  
8 error, which is fed back and combined with the next input  
9 sample. The error-feedback sigma-delta modulator operates on  
10 a highly oversampled input and uses the unit delay  $z^{-1}$  as a  
11 predictor. With this basic error-feedback modulator, only a  
12 small fraction of the bandwidth can be occupied by the  
13 required signal. In addition, the circuit only operates at  
14 baseband. A larger fraction of the Nyquist bandwidth can be  
15 made available and the modulator can be tuned if a more  
16 sophisticated error predictor is employed. This requires  
17 replacing the unit delay with a prediction filter  $P(z)$ . This  
18 generalized modulator is shown in Figure 10.

19       The operation of the re-quantizer can be understood by  
20 considering the transform domain description of the circuit.  
21 This is expressed as

22  
23       Equation 7:

$$\hat{X}(z) = X(z) + Q(z)(1 - P(z)z^{-1})$$

24  
25 where  $Q(z)$  is the  $z$ -transform of the equivalent noise source  
26 added by the quantizer  $q(\cdot)$ ,  $P(z)$  is the transfer function of  
27 the error predictor filter, and  $X(z)$  and  $\hat{X}(z)$  are the  
28 transforms of the system input and output respectively.  $P(z)$   
29 is designed to have unity gain and leading phase shift in

1 the bandwidth of interest. Within the design bandwidth, the  
2 term  $Q(z)(1-P(z)z^{-1})=0$  and so  $X(z) = \hat{X}(z)$ . By designing  $P(z)$   
3 to be commensurate with the system passband specifications,  
4 the in-band spectrum of the re-quantizer output will ideally  
5 be the same as the corresponding spectral region of the  
6 input signal.

7 To illustrate the operation of the system consider the  
8 task of recovering a signal that occupies 10% of the  
9 available bandwidth and is centered at a normalized  
10 frequency of 0.3Hz. The stopband requirement is to provide  
11 60 dB of attenuation. Figure 11A shows the input test  
12 signal. It comprises an in-band component and two out-of-  
13 band tones that are to be rejected. Figure 11B is a  
14 frequency domain plot of the signal after it has been re-  
15 quantized to 4 bits of precision by a  $\Sigma\Delta$  modulator employing  
16 an 8th order predictor in the feedback path. Notice that the  
17 60dB dynamic range requirement is supported in the bandwidth  
18 of interest, but that the out-of-band SNR has been  
19 compromised. This is of course acceptable, since the  
20 subsequent filtering operation will provide the necessary  
21 rejection. A 160-tap filter  $H(z)$  satisfies the problem  
22 specifications. The frequency response of  $H(z)$  using 12-bit  
23 filter coefficients is shown in Figure 11C. Finally,  $H(z)$  is  
24 applied to the reduced sample precision data stream  $\hat{X}(z)$  to  
25 produce the spectrum shown in Figure 11D. Observe that the  
26 desired tone has been recovered, the two out-of-band  
27 components have been rejected, and that the in-band dynamic  
28 range meets the 60 dB requirement.

29  
30 Prediction Filter Design

1        The design of the error predictor filter is a signal  
2 estimation problem. The optimum predictor is designed from a  
3 statistical viewpoint. The optimization criterion is based  
4 on the minimization of the mean-squared error. As a  
5 consequence, only the second-order statistics  
6 (autocorrelation function) of a stationary process are  
7 required in the determination of the filter. The error  
8 predictor filter is designed to predict samples of a band-  
9 limited

10 white noise process  $N_{xx}(\omega)$  shown in Figure 12.

11  $N_{xx}(\omega)$  is defined as:

12  
13 Equation 8:

$$N_{xx}(\omega) = \begin{cases} 1 & -\theta \leq \omega \leq \theta \\ 0 & \text{otherwise} \end{cases}$$

14  
15  
16 and related to the autocorrelation sequence  $r_{xx}(m)$  by  
17 discrete-time Fourier transform (DTFT).

18  
19 Equation 9:

$$N_{xx}(\omega) = \sum_{n=-\infty}^{\infty} r_{xx}(n) e^{-j\omega n}$$

20  
21  
22  
23 The autocorrelation function  $r_{xx}(n)$  is found by taking the  
24 inverse DTFT of the equation immediately above.

25  
26 Equation 10:

$$r_{xx}(n) = \frac{1}{2\pi} \int_{-\pi}^{\pi} N_{xx}(\omega) e^{-j\omega n} d\omega$$

27  
28  
29

1     $N_{xx}(\omega)$  is non-zero only in the interval  $-\theta \leq \omega \leq \theta$  giving  $r_{xx}(n)$   
2    as:

3    Equation 11:

4                      
$$r_{xx}(n) = \frac{\theta}{\pi} \text{sinc}(\theta n)$$

5

6                      So the autocorrelation function corresponding to a band-  
7    limited white noise power spectrum is a sinc function. Samples  
8    of this function are used to construct an autocorrelation  
9    matrix which is used in the solution of the normal equations  
10   to find the required coefficients. Leaving out the scaling  
11   factor in the immediately above equation, the required  
12   autocorrelation function  $r_{xx}(n)$ , truncated to p samples, is  
13   defined as:

14

15                      Equation 12:

16

17

$$r_{xx} = \frac{\sin(n\theta)}{n\theta} \quad n = 0, \dots, p-1$$

18                      The normal equations are defined as:

19    Equation 13:

20

$$r_{xx}(m) = \sum_{k=1}^p a(k) r_{xx}(m-k) \quad m = 1, 2, \dots, p$$

21

22

23                      This system of equations can be compactly written in  
24    matrix form by first defining several matrices.

25                      To design a p-tap error predictor filter first compute a  
26    sinc function consisting of p+1 samples and construct the  
27    autocorrelation matrix  $R_{xx}$  as:

28    Equation 14:

$$R_{xx} = \begin{bmatrix} r_{xx}(0) & r_{xx}(1) & \dots & r_{xx}(p-1) \\ r_{xx}(1) & r_{xx}(0) & \dots & r_{xx}(p-2) \\ \vdots & \vdots & \ddots & \vdots \\ \vdots & \vdots & \ddots & \vdots \\ r_{xx}(p-1) & r_{xx}(p-2) & \dots & r_{xx}(0) \end{bmatrix}$$

6

7

8 Next, define a filter coefficient row-vector A as:

9 Equation 15;

$$A = [a(0), a(1), \dots, a(p-1)]$$

10

11

12 where  $a(i)$ ,  $i=0, \dots, p-1$ , are the predictor filter

13 coefficients. Let the row-vector  $R'_{xx}$  be defined as:

14 Equation 16:

$$R'_{xx} = [r_{xx}(1), r_{xx}(2), \dots, r_{xx}(p)]$$

15

16 The matrix equivalent of equation 13 is:

17 Equation 17:

$$R_{xx} A^T = (R'_{xx})^T$$

18

19 The filter coefficients are therefore given as:

20

21 Equation 18:

22

$$A^T = R_{xx}^{-1} (R'_{xx})^T$$

23

24 For the case in-hand, the solution of equation 18 is an  
25 ill-conditioned problem. To arrive at a solution for A, a  
26 small constant  $\varepsilon$  is added to the elements along the diagonal

1 of the autocorrelation matrix  $R_{xx}$  in order to raise its  
2 condition number. The actual autocorrelation matrix used to  
3 solve for the predictor filter coefficients is:

4  
5 Equation 19:  
6

$$R_{xx} = \begin{bmatrix} r_{xx}(0)+\epsilon & r_{xx}(1) & \dots & r_{xx}(p-1) \\ r_{xx}(1) & r_{xx}(0)+\epsilon & \dots & r_{xx}(M-2) \\ \vdots & \vdots & \ddots & \vdots \\ r_{xx}(p-1) & r_{xx}(p-2) & \dots & r_{xx}(0)+\epsilon \end{bmatrix} \quad \begin{array}{l} 7 \\ 8 \\ 9 \\ 10 \\ 11 \\ 12 \end{array}$$

13 Bandpass Predictor Filter

14 The previous section described the design of a lowpass  
15 predictor. In this section, bandpass processes are considered.

16 A bandpass predictor filter is designed by modulating a  
17 lowpass prototype sinc function to the required center  
18 frequency  $\theta_0$ . The bandpass predictor coefficient  $h_{BP}(n)$  is  
19 obtained from the prototype lowpass sinc function  $h_{LP}(n)$  as:  
20 Equation 20:

$$21 \quad \text{sinc}_{BP}(n) = \text{sinc}_{LP}(n) \cos(\theta_0(n-k)) \quad n=0, \dots, 2p$$

22

$$23 \quad \text{where } k = \left[ \frac{2p+1}{2} \right].$$

24  
25 Highpass Predictor Filter

26 A highpass predictor filter is designed by highpass  
27 modulating a lowpass prototype sinc function to the required  
28 corner frequency  $\theta_c$ . The highpass predictor coefficients  $h_{HP}(n)$

1 are obtained from the prototype lowpass sinc function  $h_{LP}(n)$   
2 as:

3 Equation 21:  $\text{sinc}_{HP}(n) = \text{sinc}_{LP}(n) (-1)^{n-k} \quad n = 0, \dots, 2p$   
4

5

6  $\Sigma\Delta$  Modulator FPGA Implementation

7 The most challenging aspect of implementing the data  
8 modulator is producing an efficient implementation for the  
9 prediction filter  $P(z)$ . The desire to support high-sample  
10 rates, and the requirement of zero latency for  $P(z)$ , will  
11 preclude bit-serial methods from this problem. In addition,  
12 for the sake of area efficiency, parallel multipliers that  
13 exploit one time-invariant input operand (the filter  
14 coefficients) will be used, rather than general variable-  
15 variable multipliers. The constant-coefficient multiplier  
16 (KCM) is based on a multi-bit inspection version of Booth's  
17 algorithm. Partitioning the input variable into 4-bit  
18 nibbles is a convenient selection for the Xilinx Virtex  
19 function generators (FG). Each FG has 4 inputs and can be  
20 used for combinatorial logic or as application RAM/ROM. Each  
21 logic slice in the Virtex logic fabric comprises 2 FGs, and  
22 so can accommodate a  $16 \times 2$  memory slice. Using the rule of  
23 thumb that each bit of filter coefficient precision  
24 contributes 5 dB to the sidelobe behavior, 12-bit precision  
25 is used for  $P(z)$ . 12-bit precision will also be employed for  
26 the input samples. There are 3 4-bit nibbles in each input  
27 sample. Concurrently, each nibble addresses independent  $16 \times$   
28  $16$  lookup tables (LUTs). The bit growth incorporated here  
29 allows for worst case filter coefficient scaling in  $P(z)$ . No

1 pipeline stages are permitted in the multipliers because of  
2  $P(z)$ 's location in the feedback path of the modulator.

3 It is convenient to use the transposed FIR filter for  
4 constructing the predictor. This allows the adders and delay  
5 elements in the structure to occupy a single slice. 64  
6 slices are required to build the accumulate-delay path. The  
7 FPGA logic requirements for  $P(z)$ , using a 9-tap predictor,  
8 is  $\Gamma(P(z)) = 9 \times 40 + 64 = 424$  CLBs. A small amount of  
9 additional logic is required to complete the entire  $\Sigma\Delta$   
10 modulator. The final slice count is 450. The entire  
11 modulator comfortably operates with a 113 MHz clock. This  
12 clock frequency defines the system sample rate, so the  
13 architecture can support a throughput of 113 MSamples per  
14 second. The critical path through this part of the design is  
15 related to the exclusion of pipelining in the multipliers.  
16

17 Reduced Complexity FIR Mechanization

18 Now that the input signal is available as a reduced  
19 precision sample stream, filtering can be performed using  
20 area-optimized hardware. For the reasons discussed above, 4-  
21 bit data samples are a convenient match for Virtex devices.  
22 Figure 13 shows the structure of the reduced complexity FIR  
23 filter. The coded samples  $\hat{x}(n)$  are presented to the address  
24 inputs of  $N$  coefficient LUTs. In accordance with the  
25 modulated data stream precision, each LUT stores the 16  
26 possible scaled coefficient values for one tap as shown in  
27 Figure 14. An  $N$ -tap filter requires  $N$  such elements. The  
28 outputs of the minimized multipliers are combined with an  
29 add-delay datapath to produce the final result. The logic  
30 requirement for the filter is  $\Gamma(H(z)) = N\Gamma(MUL) + (N-1)\Gamma(ADD\_z^{-1})$   
31 where  $\Gamma(MUL)$  and  $\Gamma(ADD\_z^{-1})$  are the FPGA area cost functions

1 for a KCM multiplier and an add-delay datapath component  
2 respectively.

3 Using full-precision input samples without any  $\Sigma\Delta$   
4 encoding, each KCM would occupy 40 slices. The total cost of  
5 a direct implementation of  $H(z)$  is 7672 slices. The reduced  
6 precision KCMs used to process the encoded data each consume  
7 only 8 slices. Including the sigma-delta modulator the slice  
8 count is 3002 for the  $\Sigma\Delta$  approach. So the data re-  
9 quantization approach consumes only 39% of the logic  
10 resources of a direct implementation.

11

12  $\Sigma\Delta$  Decimators

13 The procedure for re-quantizing the source data can  
14 also be used effectively in an m:1 decimation filter. An  
15 interesting problem is presented when high input sample  
16 rates ( $\geq 150$  MHz) must be supported in FPGA technology. High-  
17 performance multipliers are typically realized by  
18 incorporating pipelining in the design. This naturally  
19 introduces some latency in to the system. The location of  
20 the predictor filter  $P(z)$  requires a zero-latency design.  
21 (It is possible that the predictor could be modified to  
22 predict samples further ahead in the time series, but this  
23 potential modification will not be dealt with in the limited  
24 space available.) Instead of re-quantizing, filtering and  
25 decimating, which would of course require a  $\Sigma\Delta$  modulator  
26 running at the input sample rate, this sequence of  
27 operations is re-ordered to permit several slower modulators  
28 to be used in parallel. The process is performed by first  
29 decimating the signal, re-quantizing and then filtering. Now

1 the  $\Sigma\Delta$  modulators operate at the reduced output sample rate.  
2 This is depicted in Figure 15. To support arbitrary center  
3 frequencies, and any arbitrary, but integer, down-sampling  
4 factor  $m$ , the bandpass decimation filter employs complex  
5 weights. The filter weights are of course just the bandpass  
6 modulated coefficients of a lowpass prototype filter  
7 designed to support the bandwidth of the target signal.  
8 Samples are collected from the A/D and alternated between  
9 the two modulators. Both modulators are identical and use  
10 the same predictor filter coefficients. The re-quantized  
11 samples are processed by an  $m:1$  complex polyphase filter to  
12 produce the decimated signal. Several design options are  
13 presented once the signal has been filtered and the sample  
14 rate lowered. Figure 15 illustrates one possibility. Now  
15 that the data rate has been reduced, the low rate signal is  
16 easily shifted to baseband with a simple, and area  
17 efficient, complex heterodyne. One multiplier and a single  
18 digital frequency synthesizer could be time shared to  
19 extract one or multiple channels.

20 It is interesting to investigate some of the changes  
21 that are required to support the  $\Sigma\Delta$  decimator. The center  
22 frequency of the prediction filter should be designed to  
23 predict samples in the required spectral region in  
24 accordance with the output sample rate. For example,  
25 consider  $m=2$ , and the required channel center frequency  
26 located at 0.1 Hz, normalized with respect to the input  
27 sample rate. The prediction filter should be designed with a  
28 center frequency located at 0.2 Hz. In addition, the quality  
29 of the prediction should be improved. With respect to the  
30 output sample rate, the predictors are required to operate

1 over a wider fractional bandwidth. This implies more filter  
2 coefficients in  $P(z)$ . The increase in complexity of this  
3 component should be balanced against the savings that result  
4 in the reduced complexity filter stage to confirm that a net  
5 savings in logic requirements is produced. To more clearly  
6 demonstrate the approach, consider a 2:1 decimator, a  
7 channel center frequency at 0.2 Hz and a 60 dB dynamic range  
8 requirement.

9 Figure 16(a) shows the double-sided spectrum of the  
10 input test signal. The input signal is commutated between  $\Sigma\Delta_0$   
11 and  $\Sigma\Delta_1$  to produce the two low-precision sequences  $\hat{x}_0(n)$  and  
12  $\hat{x}_1(n)$ . The respective spectrums of these two signals are shown  
13 in Figures 16(b) and 16(c). The complex decimation filter  
14 response is defined in Figure 16(d). After filtering, a  
15 complex sample stream supported at the low output sample  
16 rate is produced. This spectrum is shown in Figure 16(e).  
17 Observe that the out-of-band components in the test signal  
18 have been rejected by the specified amount and that the in-  
19 band data meets the 60 dB dynamic range requirement. For  
20 comparison, the signal spectrum resulting from applying the  
21 processing stages in the order, re-quantize, filter and  
22 decimate is shown in Figure 16(f). The interesting point to  
23 note is that while the dual  $\Sigma\Delta$  modulator approach satisfies  
24 the system performance requirements, its out-of-band  
25 performance is not quite as good as the response depicted in  
26 Figure 16(f). The stopband performance of the dual modulator  
27 architecture has degraded by approximately 6 dB. This can be  
28 explained by noting that the shaping noise produced by each  
29 modulator is essentially statistically independent. Since  
30 there is no coupling between these two components prior to

1 filtering, complete phase cancellation of the modulator  
2 noise cannot occur in the polyphase filter.

3

4 Discussion

5 To provide a frame of reference for the  $\Sigma\Delta$  decimator,  
6 consider an implementation that does not pre-process the  
7 input data, but just applies it directly to a polyphase  
8 decimation filter. A complex filter processing real-valued  
9 data consumes double the FPGA resources of a filter with  
10 real weights. For N=160, 15344 CLBs are required. This  
11 Figure is based on a cost of 40 CLBs for each KCM and 8 CLBs  
12 for an add-delay component.

13 Now consider the logic accounting for the dual  
14 modulator approach. The area cost  $\widehat{\Gamma(\text{FIR})}$  for this filter is  
15

16 Equation 22:

$$\widehat{\Gamma(\text{FIR})} = 2\widehat{\Gamma(\Sigma\Delta)} + \widehat{\Gamma(\text{MUL})} + \widehat{\Gamma(\text{ACC}_z^{-1})}$$

17  
18 where  $\widehat{\Gamma(\Sigma\Delta)}$  represents the logic requirements for one  $\Sigma\Delta$   
19 modulator, and  $\widehat{\Gamma(\text{MUL})}$  is the logic needed for a reduced  
20 precision multiplier. Using the filter specifications  
21 defined earlier, and 18-tap error prediction filters,  $\widehat{\Gamma(\text{FIR})} =$   
22  $2 \times 738 + 2 \times ((160 + 159) \times 8) = 6596$ . Comparing the area  
23 requirements of the two options produces the ratio

24

25 Equation 23:

$$\lambda = \frac{\widehat{\Gamma(\text{FIR})}}{\widehat{\Gamma(\text{FIR})}} = 6596/15344 \approx 43\%$$

26

1 So for this example, the re-quantization approach has  
2 produced a realization that is significantly more area  
3 efficient than a standard tapped-delay line implementation.

4

5 Center Frequency Tuning

6 For both the single-rate and multi-rate  $\Sigma\Delta$  based  
7 architectures, the center frequency is defined by the  
8 coefficients in the predictor filter and the coefficients in  
9 the primary filter. The constant coefficient multipliers can  
10 be constructed using the FPGA function generators configured  
11 as RAM elements. When the system center frequency is to be  
12 changed, the system control hardware would update all of the  
13 tables to reflect the new channel requirements. If only  
14 several channel locations are anticipated, separate  
15 configuration bit streams could be stored, and the FPGA(s)  
16 re-configured as needed.

17

18 Bandpass  $\Sigma\Delta$ s Using Allpass Networks

19 In an earlier section we discussed how to design a  
20 predicting filter for the feedback loop of a standard sigma  
21 delta modulator. The predicting filter increases the order  
22 of the modulator so that the modified structure has  
23 additional degrees of freedom relative to a single-delay  
24 noise feedback loop. These extra degrees of freedom have  
25 been used in two ways, first to broaden the bandwidth of the  
26 loop's noise transfer function, and second to tune its  
27 center frequency. The tuning process entailed an off line  
28 solution of the Normal equations which while not difficult,  
29 does present a small delay and the need for a background  
30 processor. We can define a sigma-delta loop with a

1 completely different architecture that offers the same  
2 flexibility, namely wider bandwidth and a tunable center  
3 frequency that does not require this background task. In  
4 this alternate architecture, a fixed set of feedback weights  
5 from a set of digital integrators defines a base-band  
6 prototype filter with a desirable NTF. The filter is tuned  
7 to arbitrary frequencies by attaching to each delay element  
8  $z^{-1}$ , a simple sub-processing element that performs a base-  
9 band to band-pass transformation of the prototype filter.  
10 This processing element tunes the center frequency of its  
11 host prototype with a single real and selectable scalar. The  
12 structure of a fourth order prototype sigma-delta loop is  
13 shown in Figure 17. The time and spectrum obtained by using  
14 the loop with a 4-bit quantizer is shown in Figure 18. In  
15 this structure the digital integrator poles are located on  
16 the unit circle at DC. The local feedback ( $a_1$  and  $a_2$ )  
17 separates the poles by sliding them along the unit circle,  
18 and the global feedback ( $b_1$ ,  $b_2$ ,  $b_3$  and  $b_4$ ) places these  
19 poles in the feedback path of the quantizer so they become  
20 noise transfer function zeros. These zeros are positioned to  
21 form an equal-ripple stop band for the NTF. The coefficients  
22 selected to match the NTF pole-zero locations to an elliptic  
23 high pass filter. The single sided bandwidth of this fourth  
24 order loop is approximately 4% of the input sample rate.

25 The low-pass to band-pass transformation for a sampled  
26 data filter is achieved by substituting an all-pass transfer  
27 function  $G(z)$  for the all-pass transfer function  $z^{-1}$ . This  
28 transformation is shown in equation 24.

29

30 Equation 24:

31

$$z^{-1} \longrightarrow -z^{-1} \left( \frac{1-cz}{z-c} \right)$$

1  
2       A block diagram of a digital filter with the transfer  
3       function for  $G(z)$  is shown in Figure 19. Examining the left  
4       hand block diagram, we find the transfer function from  $x(n)$   
5       to  $y(n)$  is the all-pass network  $-(1-cz)/(z-c)$ , while the  
6       transfer function from  $x(n)$  to  $v(n)$  is  $-(1/z)(1-cz)/(z-c)$ .  
7       When we absorb the external negative sign change in the  
8       internal adders of the filter we obtain the simple right-  
9       hand side version of the desired transfer function  $G(z)$ .

10       After the block diagram substitution has been made, we  
11      obtain Figure 20, the tunable version of the low-pass  
12      prototype. The basic structure of the prototype remains the  
13      same when we replace the delay with the tunable all-pass  
14      network. The order of the filter is doubled by the  
15      substitution since each delay is replaced by a second order  
16      sub-filter. Tuning is trivially accomplished by changing the  
17      c multiplier of the all-pass network. The tuned version of  
18      the system reverts back to the prototype response if we set  
19      c to 1.

20       Figure 21 presents the time and spectrum obtained by  
21      using the tunable loop with a 4-bit quantizer shown in  
22      Figure 20. The single sided bandwidth of the prototype  
23      filter is distributed to the positive and negative spectral  
24      bands of the tuned filter. Thus the two-sided bandwidth of  
25      each spectral band is approximately 4% of the input sample  
26      rate.

27       We now estimate the computational workload required to  
28      operate the prototype and tunable filter. The prototype

1 filter has six coefficients to form the 4-poles and the 4-  
2 zeros of the transfer function. The two  $a_k$   $k=0,1$  coefficients  
3 determine the four zero locations. These are small  
4 coefficients and can be set to simple binary scalers. The  
5 values computed for this filter for  $a_1$  and  $a_2$  were 0.0594 and  
6 0.0110. These can be approximated by 1/16 and 1/128, which  
7 lead to no significant shift of the spectral zeros in the  
8 NTF. These simple multiplications are virtually free in the  
9 FPGA hardware since they are implemented with suitable  
10 wiring. The four coefficients  $b_k$   $k=0,\dots,3$  are 1.000, 0.6311,  
11 0.1916, and 0.0283 respectively were replaced with  
12 coefficients containing one or two binary symbols to obtain  
13 values 1.000,  $1/2+1/8$  (0.625),  $1/8+1/16$  (0.1875) and  $1/32$   
14 (0.03125). When the sigma-delta loop ran with these  
15 coefficients there was no discernable change in bandwidth or  
16 attenuation level of the loop. The loop operates equally as  
17 well in the tuning mode and the non-tuning mode with the  
18 approximate coefficients listed above. Thus the only real  
19 multiplies in the tunable sigma-delta loop are the c  
20 coefficients of the all-pass networks. These networks are  
21 unconditionally stable and always exhibit all-pass behavior  
22 even in the presence of finite arithmetic and finite  
23 coefficients. This is because the same coefficient forms the  
24 numerator and the denominator. Errors in approximating the  
25 coefficients for c simply result in a frequency shift of the  
26 filter's tuned center. The c coefficient is determined from  
27 the cosine of the center frequency (in radians/sample). The  
28 curve for this relationship is shown in Figure 22. Also  
29 shown is an error due to approximating c by  $c+\delta c$ . The  
30 question is, what is the change in center frequency  $\theta$ , from

1    $\theta + \delta\theta$  due to the approximation of  $c$ ? We can see that the slope  
2   at the operating point on the cosine curve is  $-\sin\theta$  so that  
3    $\delta c / \delta\theta \approx -\sin(\theta)$  so that  $\delta c \approx -\delta\theta\sin(\theta)$  is the required  
4   precision to maintain a specified error. We note that tuning  
5   sensitivity is most severe for small frequencies where  $\sin(\theta)$   
6   is near zero. The tolerance term,  $\delta\theta\sin(\theta)$ , is quadratic for  
7   small frequencies, but the lowest frequency that can be  
8   tuned by the loop is half the NTF pass-band bandwidth. For  
9   the fourth order system described here, this bandwidth is 4%  
10   of the sample rate, so the half-bandwidth angle is 2%, or  
11   0.126 radians. To assure that the frequency to which the  
12   loop is tuned has an error smaller than 1% of center  
13   frequency,  $\delta c < \delta\theta\sin(\theta) \Rightarrow \delta c < (0.126/100)(0.126) = 0.0002$ ,  
14   which corresponds to a 14 bit coefficient. An error of less  
15   than 10% center frequency can be achieved with 10 bit  
16   coefficients.

17   The tuning} multipliers could be implemented as full  
18   multipliers in the FPGA hardware or as dynamically re-  
19   configured KCMs, or KDCM, as shown in Figure 23. The later  
20   approach conserves FPGA resources at the expense of  
21   introducing a start-up penalty each time the center  
22   frequency is changed. The start-up period is the  
23   initialization time of the KCM LUT. When a new center  
24   frequency is desired, the tuning constant is presented to  
25   the k input of the KDCM and the load signal LD is asserted.  
26   This starts the initialization engine, which requires 16  
27   clock cycles to initialize 16 locations in the multiplier  
28   LUT. The initialization engine relies on the automatic shift  
29   mode of the Virtex LUTs. In this mode of operation a LUT's  
30   register contents are passed from one cell to the next cell

1 on each clock tick. This avoids the requirement for a  
2 separate address generator and multiplexor in the  
3 initialization hardware. Observe from Figure 23 that the  
4 initialization engine only introduces a small amount of  
5 additional hardware over that of a static KCM.

6 There is approximately a factor of 4 difference in the  
7 area of a KDCM and full multiplier.  
8

9  $\Sigma\Delta$  DC Canceler

10 Unwanted DC components can be introduced into a DSP  
11 datapath at several places. It may be presented to the  
12 system via an un-trimmed offset in the analog-to-digital  
13 conversion pre-processing circuit, or may be attributed to  
14 bias in the A/D converter itself. Even if the sampled input  
15 signal has a zero mean, DC content can be introduced through  
16 arithmetic truncation processes in the fixed-point datapath.  
17 For example, in a multi-stage multi-rate filter, the  
18 intermediate filter output samples may be quantized between  
19 stages in order to compensate for the filter processing gain  
20 and thereby keep the word-length requirements manageable.  
21 The introduced DC bias can impact the dynamic range  
22 performance of a system and potentially increase the error  
23 rate in a digital receiver application.

24 In a fixed-point datapath, the bias can cause  
25 unnecessary saturation events that would not occur if the DC  
26 was not present in the system. In a digital communication  
27 receiver employing M-ary QAM modulation, the DC bias can  
28 interfere with the symbol decision process, so causing  
29 incorrect decoding and therefore increasing the bit error  
30 rate.

1        In some cases the introduced bias can be ignored and is  
2 of no concern. However, for other applications it is  
3 desirable to remove the DC component.

4        One solution to removing the unwanted DC level is to  
5 employ a DC canceler. A simple canceler is shown in Figure  
6 24. It is easy to show that the transfer function of the  
7 network is

8

9        Figure 25:

$$H(z) = \frac{z-1}{z-(1-z)}$$

10  
11  
12      The cancellation is due to the transfer function zero at 0  
13 Hz. The pole at  $1-\mu$  controls the system bandwidth, and hence  
14 the system transient response. The location of the zero at  
15  $z=1$  removes the DC  
16 component in the signal, but there are some problems with a  
17 practical implementation of this circuit.

18      Figure 25A is a spectral domain representation of a  
19 biased signal presented to the DC canceler. Figure 25B is  
20 the processed signal spectrum at  $y_q(n)$  in Figure 24. We  
21 observe that the DC content in the input signal has been  
22 completely removed. However, in the process of running the  
23 canceling loop the network processing gain has caused a  
24 dynamic range expansion. So although the sample stream  $y_q(n)$   
25 is a zero mean process, it requires a larger number of bits  
26 to represent each sample than is desirable. The only option  
27 with the circuit is to re-quantize  $y_q(n)$  to produce  $y(n)$   
28 using the quantizer  $Q(\cdot)$ . The effect of this operation is

1 shown in Figure 25C, which demonstrates, not surprisingly,  
2 that after an 8-bit quantizer, the signal now has a DC  
3 component and we are almost back to where we started. How  
4 can the canceler be re-organized to avoid this  
5 implementation pitfall? One option is to embed the re-  
6 quantizer in the feedback loop in the form of a  $\Sigma\Delta$  modulator  
7 as shown in Figure 26. The modulator can be a very simple  
8 1st order loop such as the error feedback  $\Sigma\Delta$  modulator shown  
9 in Figure 9. Figure 25D demonstrates the operation of the  
10 circuit for 8-bit output data. Observe from the Figure that  
11 the DC has been removed from the signal while employing the  
12 same 8-bit output sample precision that was used in Figure  
13 24. The simple  $\Sigma\Delta$ M  
14 employed in the canceler is easily implemented in an FPGA.  
15

16 Simplify Digital Receiver Control Loops Using  $\Sigma\Delta$  Modulators

17 In earlier sections we recognized that when a sampled  
18 data input signal has a bandwidth that is a small fraction  
19 of its sample rate the sample components from this  
20 restricted bandwidth are highly correlated. We took  
21 advantage of that correlation to use a digital sigma-delta  
22 modulator to requantize the signal to a reduced number of  
23 bits. The sigma-delta modulator encodes the input signal  
24 with a reduced number of bits while preserving full input  
25 precision over the signal bandwidth by placing the increased  
26 noise due to requantization in out-of-band spectral  
27 positions that are already scheduled to be rejected by  
28 subsequent DSP processing. The purpose of this  
29 requantization is to allow the subsequent DSP processing to  
30 be performed with reduced arithmetic resource requirements

1 since the desired data is now represented by a smaller  
2 number of bits.

3 A similar remodulation of data samples can be employed for signals generated within a DSP process when the bandwidth of the signals are small compared to the sample rate of the process. A common example of this circumstance is the generation of control signals used in feedback paths of a digital receiver. These control signals include a gain control signal for a voltage controlled amplifier in an automatic gain control (AGC) loop and VCO (voltage controlled oscillator) control signals in carrier recovery and timing recovery loops. A block diagram of a receiver with these specific controls signals is shown in Figure 27. The control signals are generated from processes operating at a sample rate appropriate to the input signal bandwidth. The bandwidth of control loops in a receiver are usually a very small fraction of the signal bandwidth, which means that the control signal are very heavily oversampled. As a typical example, in a cable TV modem, the input bandwidth is 6 MHz, the processing sample rate is 20 MHz, and the loop bandwidth may be 50 kHz. For this example, the ratio of sample rate to bandwidth is 400-to-1.

23 As seen in Figure 27, the process of delivering these  
24 oversampled control signals to their respective control  
25 points entails the transfer of 16 bit words to external  
26 control registers, requiring appropriate busses, addressing,  
27 and enable lines as well as the operation of 16-bit digital-to-analog converters (DACS).

29 We can use a sigma-delta modulator to requantize the  
30 16-bit oversampled control signals in the digital receiver  
31 prior to passing them out of the processing chip. The sigma-

1 delta can preserve the required dynamic range over the  
2 signal's restricted bandwidth with a one-bit output. As  
3 suggested in Figure 28, the transfer of a single bit to  
4 control the analog components is a significantly less  
5 difficult task than the original. We no longer require  
6 registers to accept the transfer, the busses to deliver the  
7 bits, or the DAC to convert the digital data to the analog  
8 levels the data represents. All that is needed a simple  
9 filter (and likely an analog amplifier to satisfy drive  
10 level and offset requirements). Experience shows that a 1-  
11 bit, one-loop sigma-delta modulator could achieve 80 dB  
12 dynamic range and requires a single RC filter to reconstruct  
13 the analog signal. A two-loop sigma-delta modulator is  
14 required to achieve 16-bit precision for which a double RC  
15 filter is required to reconstruct the analog output signal.  
16 Figure 29 shows the time response of the one-bit two loop  
17 sigma-delta converter to a slowly varying control signal and  
18 the reconstructed signal obtained from the dual-RC filter.  
19 Figure 30 shows the spectrum obtained from a 1-bit two-loop  
20 modulator and the spectrum obtained from an unbuffered RC-RC  
21 filter.

22 This example has shown how with minimal additional  
23 hardware, an FPGA can generate analog control signals to  
24 control low-bandwidth analog functions in a system.  
25 An observation worthy of note, is that the audio engineering  
26 community has recognized the advantage offered by this  
27 option of requantizing a 16-bit oversampled data stream to  
28 1-bit data stream. In that community, the output signal is  
29 intentionally upsampled by a factor of 64 and then  
30 requantized to 1-bit in a process called a MASH converter.

1 Nearly all CD players use the MASH converter to deliver  
2 analog audio signals.

3

4 What Have We Gained?

5 What has been achieved by expressing our signal  
6 processing problems in terms of  $\Sigma\Delta M$  techniques?

7

8 The paper has demonstrated some  $\Sigma\Delta M$  techniques for the  
9 compact implementation of certain types of filter and  
10 control applications using FPGAs. This optimization can be  
11 used in several ways to bring economic benefits to a  
12 commercial design. By exploiting  $\Sigma\Delta M$  filter processes, a  
13 given processing load may be realizable in a lower-density,  
14 and hence less expensive, FPGA than is possible without  
15 access to these techniques. An alternative would be to  
16 perform more processing using the same hardware. For  
17 example, processing multiple channels in a communication  
18 system.

19 In addition to FPGA area trade-offs, the  $\Sigma\Delta M$  methods  
20 can result in reduced power consumption in a design. Power P  
21 may be expressed as

22

$$P = CV^2 f_{clk}$$

23 where C is capacitance, V is voltage and f is the system  
24 clock frequency. By reducing the silicon area requirements  
25 of a filter, we can simultaneously reduce the power  
26 consumption of the design. For the examples considered  
27 earlier, logic resource savings of greater than 50% were  
28 demonstrated. The savings is proportional to increased

1 efficiency in the system power budget, and this of course is  
2 very important for mobile applications.

3 The  $\Sigma\Delta$  AGC, timing and carrier recovery control loop  
4 designs are also important examples in a industrial context.  
5 The examples illustrated how the component count in a mixed  
6 analog/digital system can be reduced. In fact, not only is  
7 the component count reduced, but printed circuit board area  
8 is minimized. This results in more reliable and physically  
9 smaller implementations. The reduced component count also  
10 results in reduced power consumption. In addition, since the  
11 control loops no longer require wide output buses from the  
12 FPGA to multi-bit DACs that generate analog control  
13 voltages, power consumption is decreased because fewer FPGA  
14 I/O pads are being driven.

15  
16 References

17 The subject matter of this application is excerpted  
18 from and article entitled "FPGA Signal Processing Using  
19 Sigma-Delta Modulation," C. H. Dick and F. J. Harris, IEEE  
20 Signal Processing Magazine (January 2000), which is  
21 incorporated herein by reference. The following documents  
22 may also be of interest, and are also incorporated by  
23 reference.

- 24 [1] Atmel, AT40K/05/10/20/40 Data Sheet, 1999.  
25 [2] J. A. C. Bingham, The Theory and Practice of Modem  
26 Design, John Wiley & Sons, New York, 1998.  
27 [3] J. C. Candy and G. C. Temes, "Oversampling Methods for  
28 A/D and D/A Conversion" in Oversampling Delta Sigma  
29 Data Converters - Theory Design and Simulation, IEEE  
30 Press, New York, 1992.

- 1 [4] M. E. Frerking, Digital Signal Processing in
- 2 Communication Systems, Van Nostrand Reinhold, New York,
- 3 1994.
- 4 [5] S. Haykin, "Modern Filters", Macmillan Publishing Co.,
- 5 New York, 1990.
- 6 [6] H. Meyr, M. Moeneclaey and S. A. Fechtal, Digital
- 7 Communication Receivers, John Wiley & Sons Inc., New
- 8 York, 1998.
- 9 [7] S. R. Norsworthy, R. Schreier and G. C. Temes, \Delta-
- 10 Sigma Data Converters", IEEE Press, Piscataway, NJ,
- 11 1997.
- 12 [8] D. A. Patterson and J. L. Hennessy, Computer
- 13 Architecture: A Quantitative Approach, Morgan Kaufmann
- 14 Publishers Inc., California, 1990.
- 15 [9] A. Peled and B. Liu, "A New Hardware Realization of
- 16 Digital Filters", IEEE Trans. on Acoust., Speech,
- 17 Signal Processing, vol. 22, pp. 456-462, Dec. 1974.
- 18 [10] J. G. Proakis, and D. G. Manolakis, Digital Signal
- 19 Processing Principles, Algorithms and Applications
- 20 Second Edition, Maxwell Macmillan International, New
- 21 York, 1992.
- 22 [11] S. A. White, "Applications of Distributed Arithmetic to
- 23 Digital Signal Processing", IEEE ASSP Magazine, Vol.
- 24 6(3), pp. 4-19, July 1989.
- 25 [12] Xilinx Inc., The Programmable Logic Data Book, 1999.

1       CLAIMS

- 2   1. A DC canceler circuit comprising:
- 3      a. a canceler input terminal adapted to receive a  
4           series of data input samples;
- 5      b. a canceler output terminal adapted to provide a  
6           series of data output samples;
- 7      c. a feedback path having:
- 8         i. a feedback-path input terminal connected to  
9               the canceler output terminal;
- 10       ii. a feedback-path output terminal connected to  
11              the canceler input terminal; and
- 12       iii. a sigma-delta modulator connected between the  
13             feedback-path input terminal and the  
14             feedback-path output terminal.

1           TUNABLE NARROW-BAND FILTER INCLUDING  
2           SIGMA-DELTA MODULATOR

3

4           Christopher H. Dick  
5           Frederic J. Harris

6

7           ABSTRACT

8         Sigma-delta modulation ( $\Sigma\Delta M$ ) techniques provide a range  
9         of opportunities in a signal processing system for both  
10       increasing performance and datapath optimization along the  
11       silicon-area axis in the design space.  $\Sigma\Delta M$  technology,  
12       together with FPGA based signal processing hardware, can be  
13       combined to produce creative, high-performance and area  
14       efficient solutions to many signal processing problems.

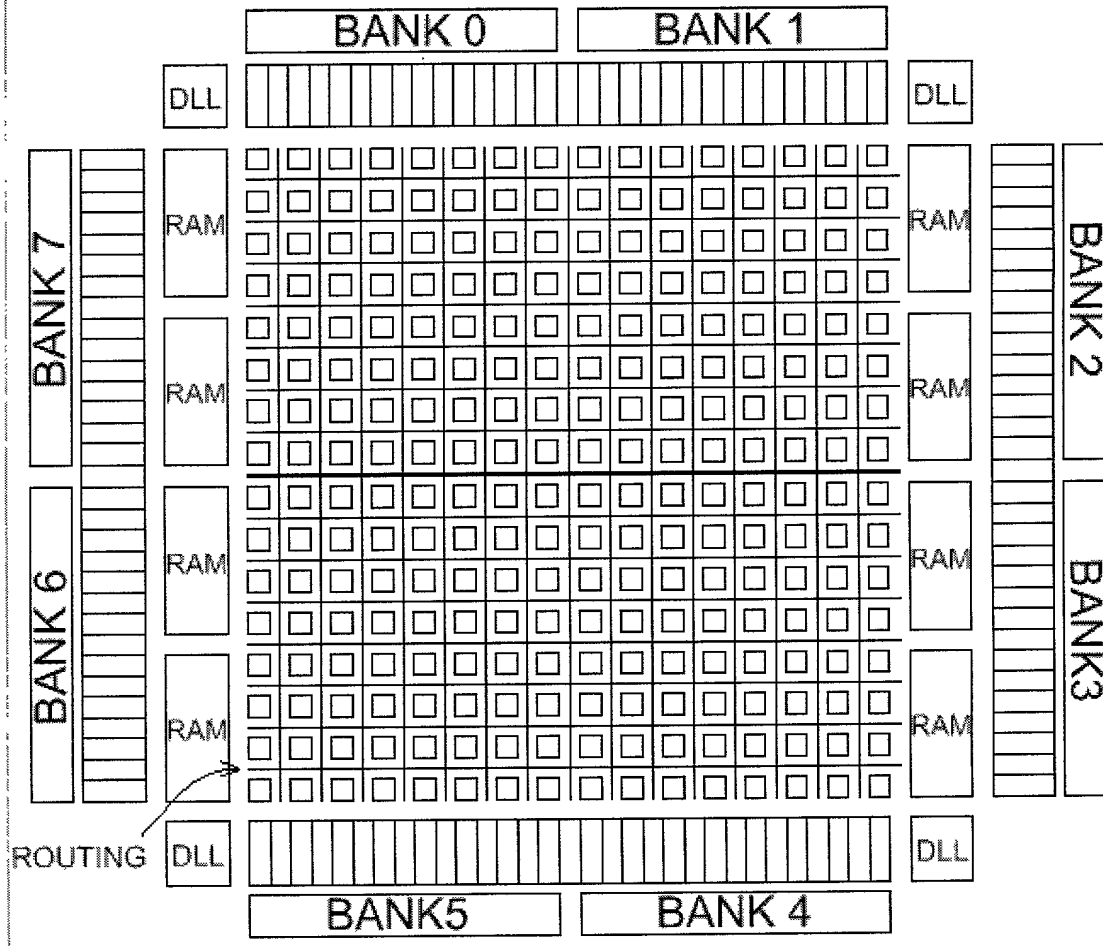


FIG. 1

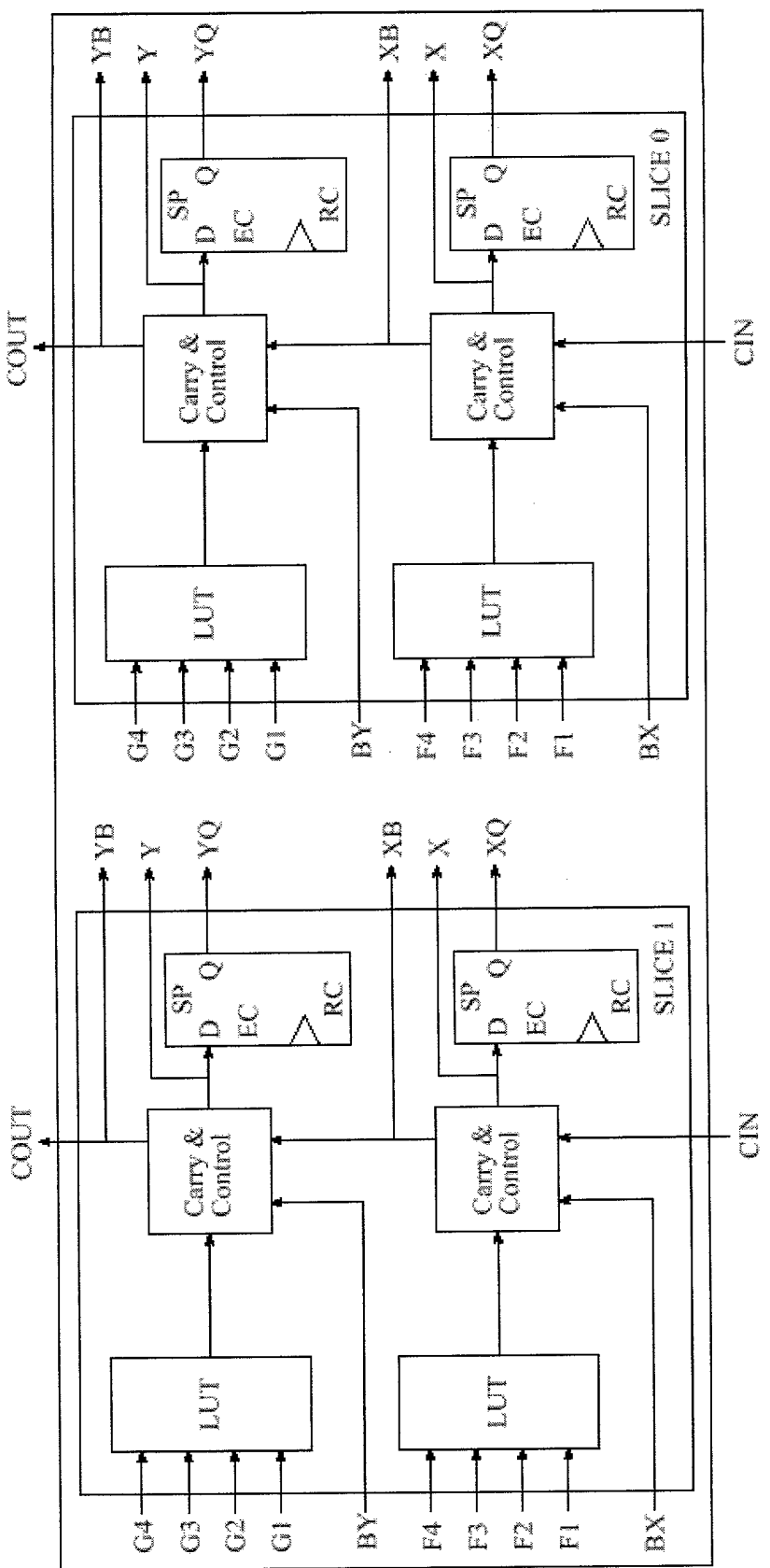
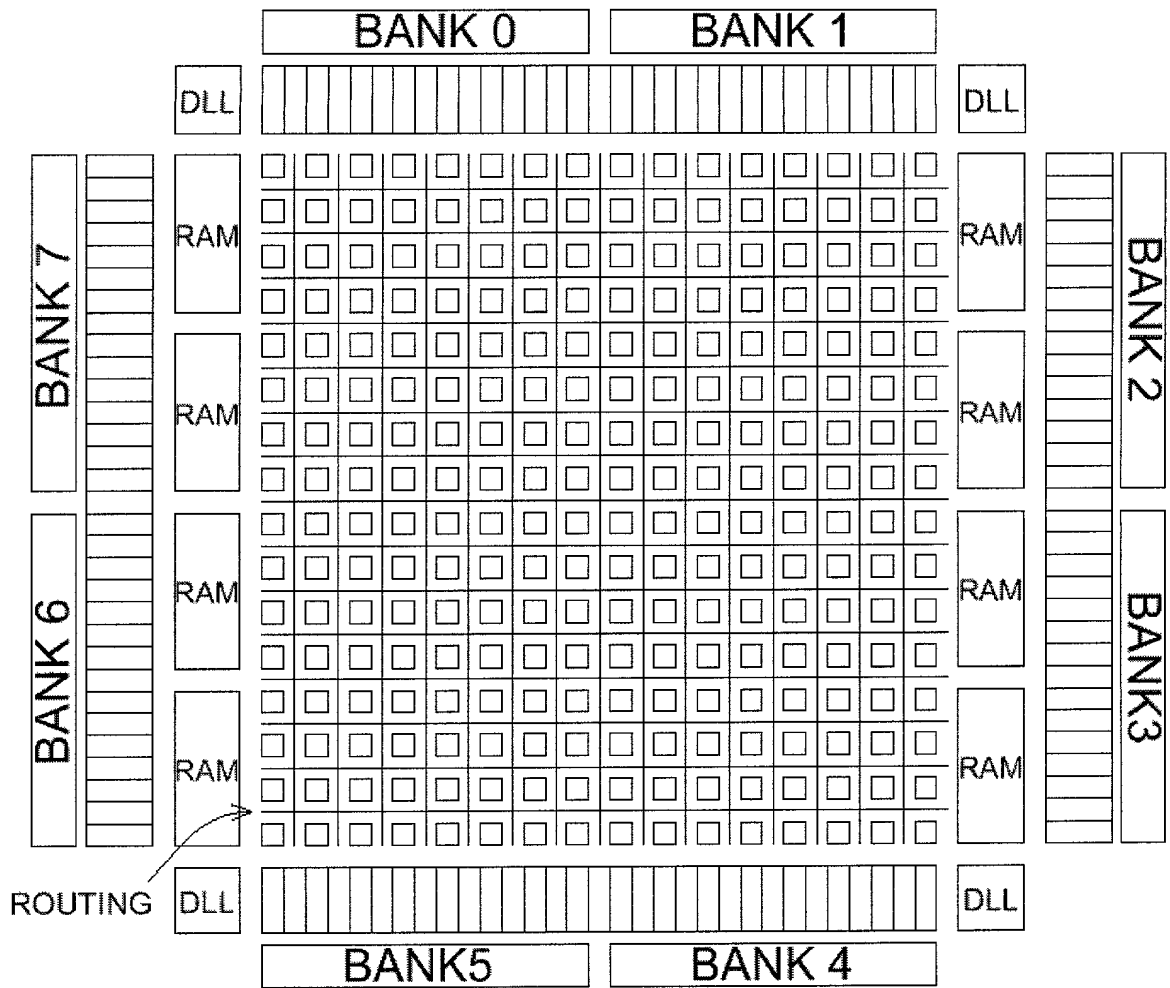


FIG. 2



DLL = DELAY LOCKED LOOP

RAM = BLOCK RAM - VARIOUS FORM FACTORS FROM  
4096x1 TO 256X16

= 2 SLICE CLB       =I/O

**BANK N** =MULTI-STANDARD I/O SUPPORT

**FIG. 3**

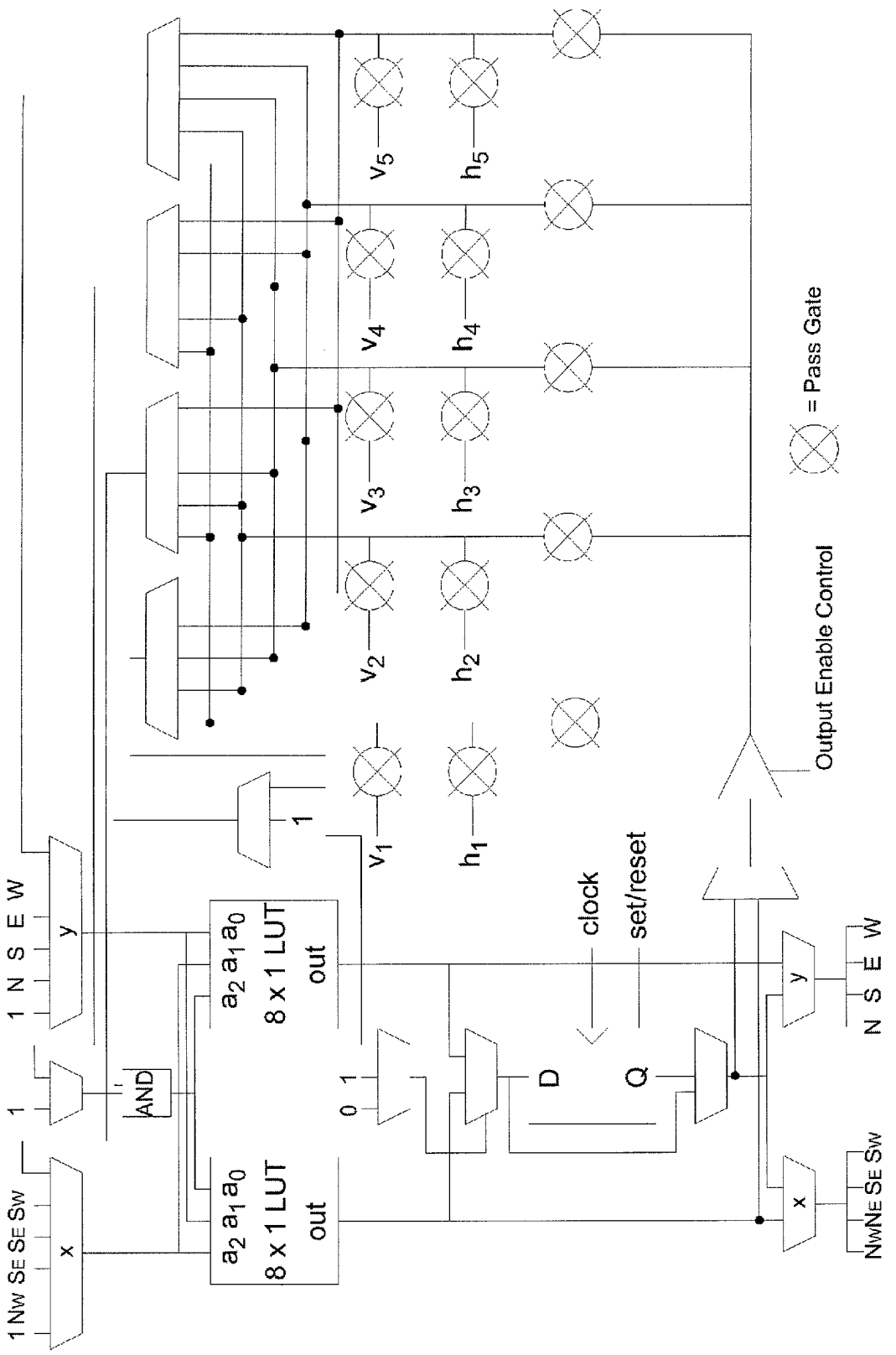


FIG. 4

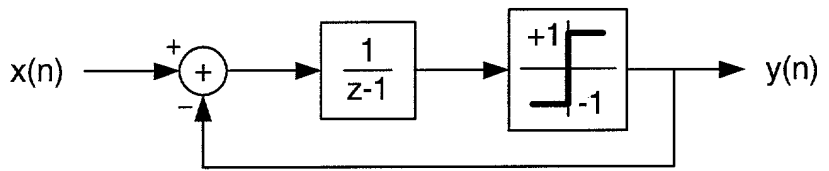


FIG. 5

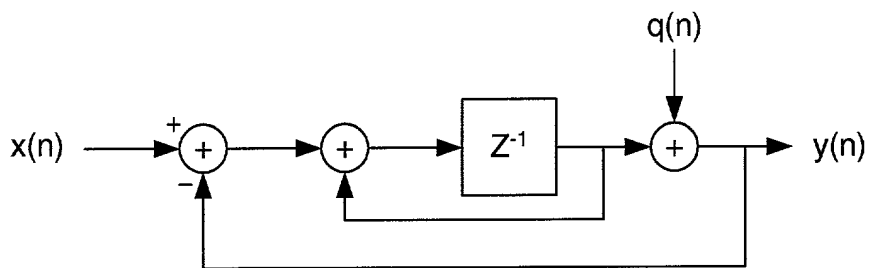


FIG. 6

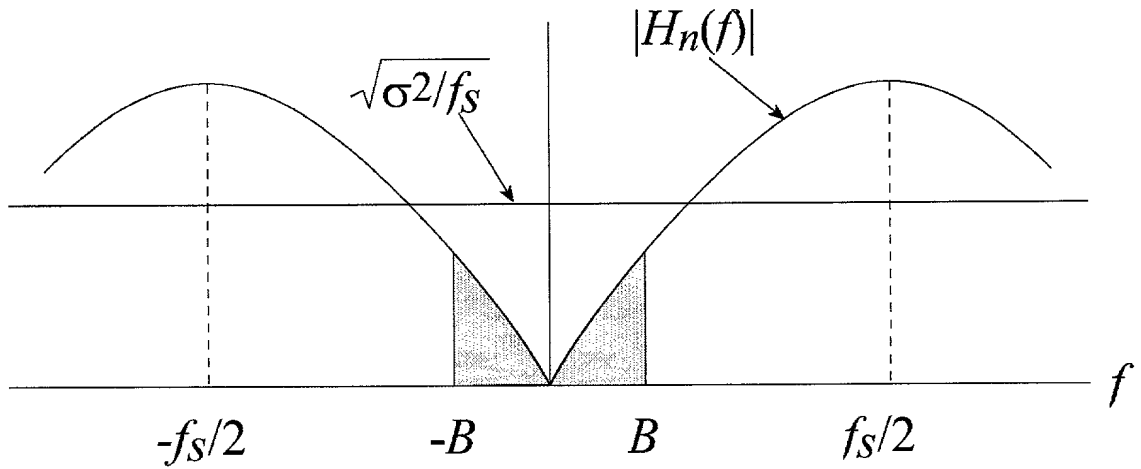


FIG. 7

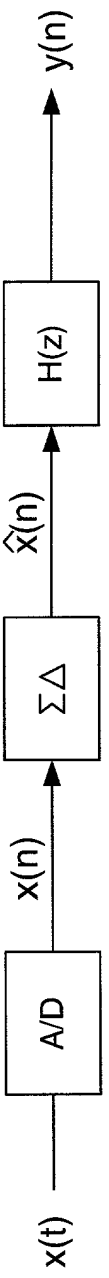


FIG. 8

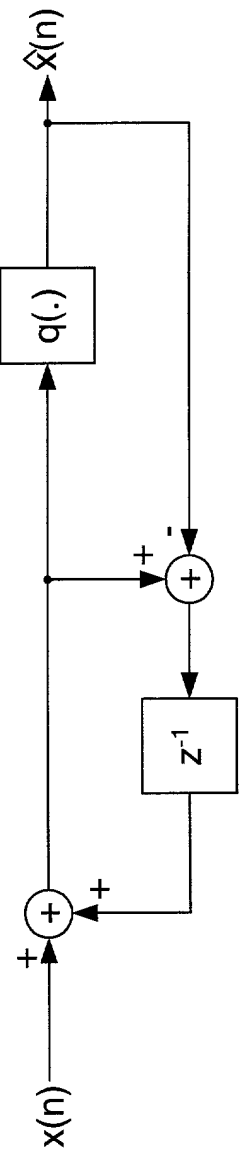


FIG. 9

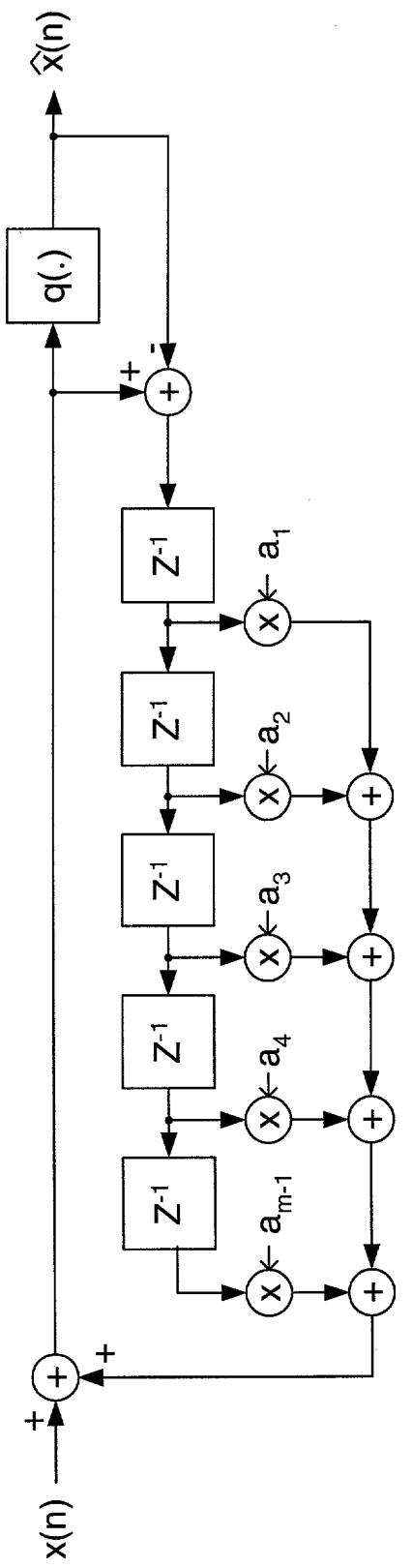


FIG. 10

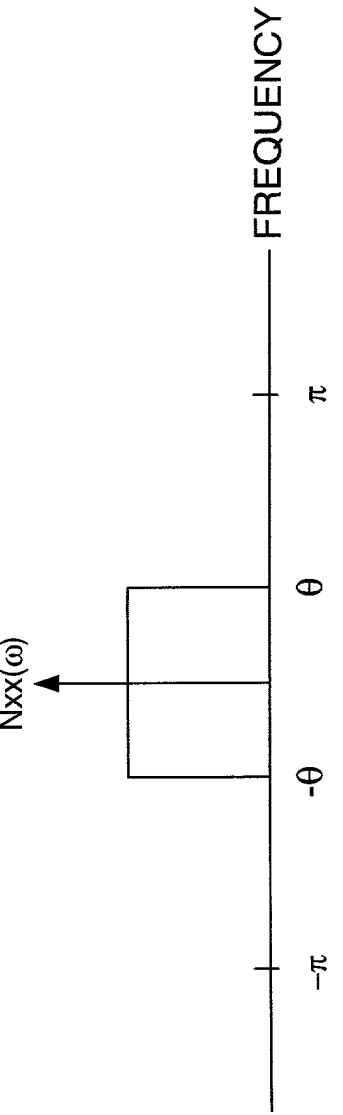


FIG. 12

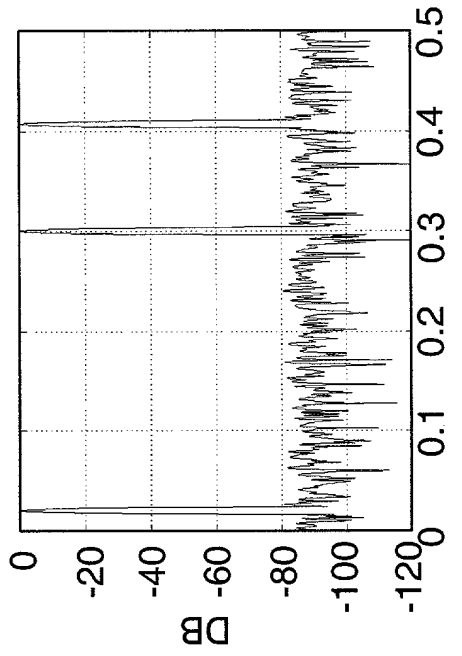


FIG. 11A

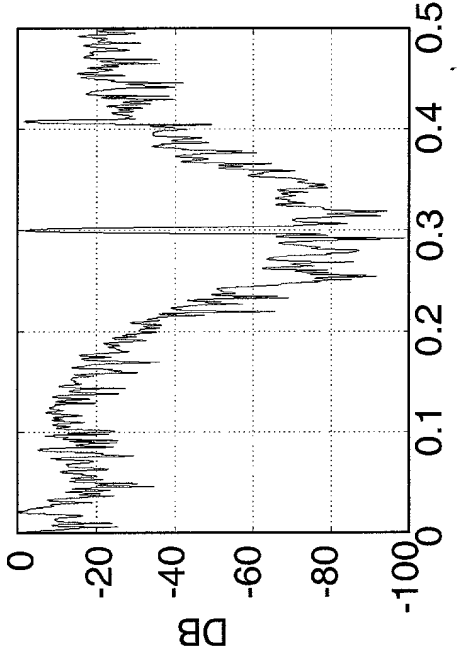


FIG. 11B

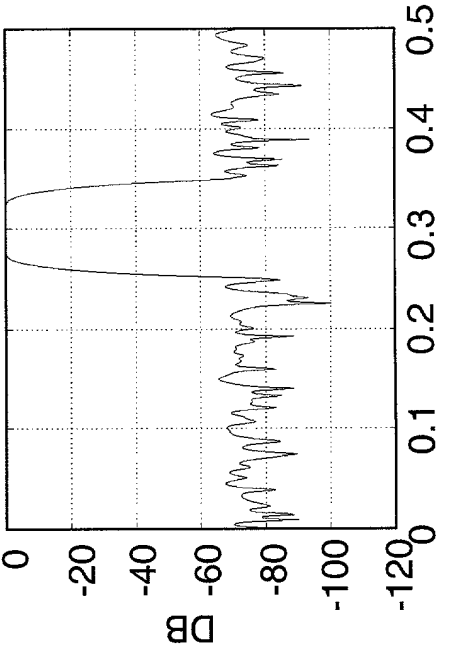


FIG. 11C

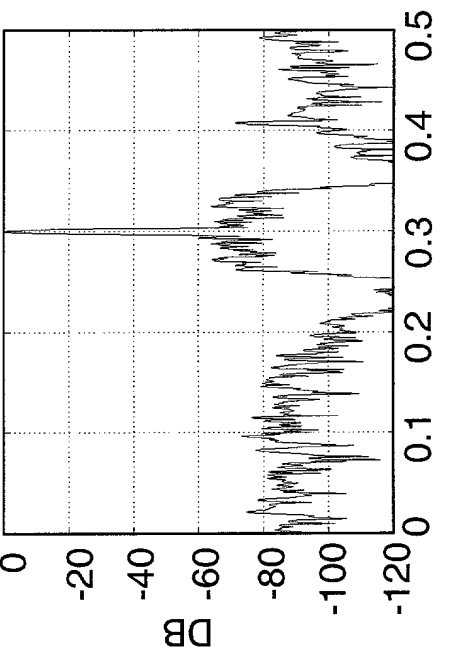


FIG. 11D

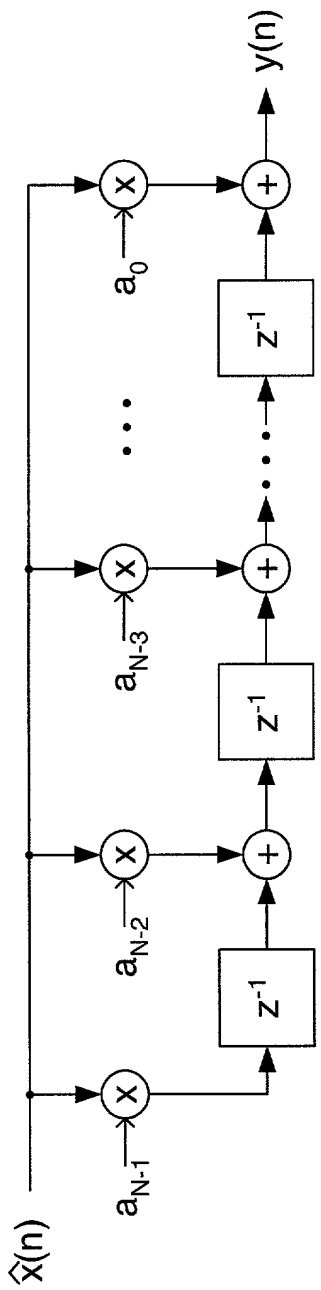


FIG. 13

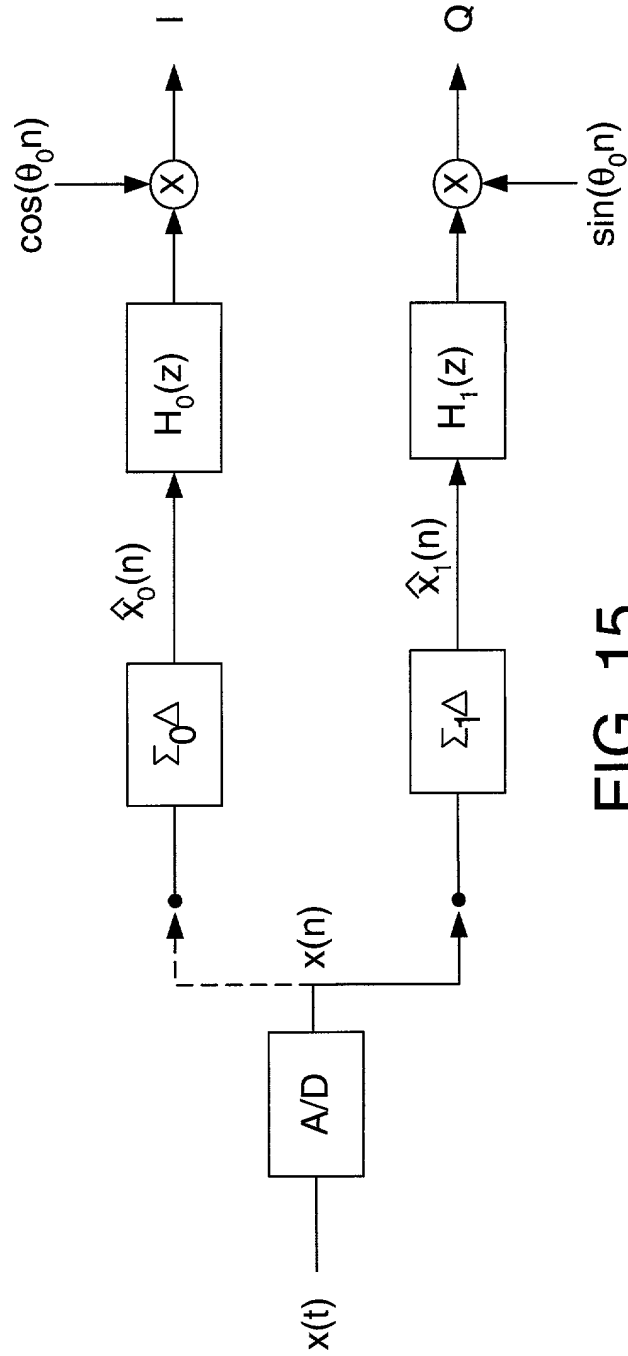


FIG. 15

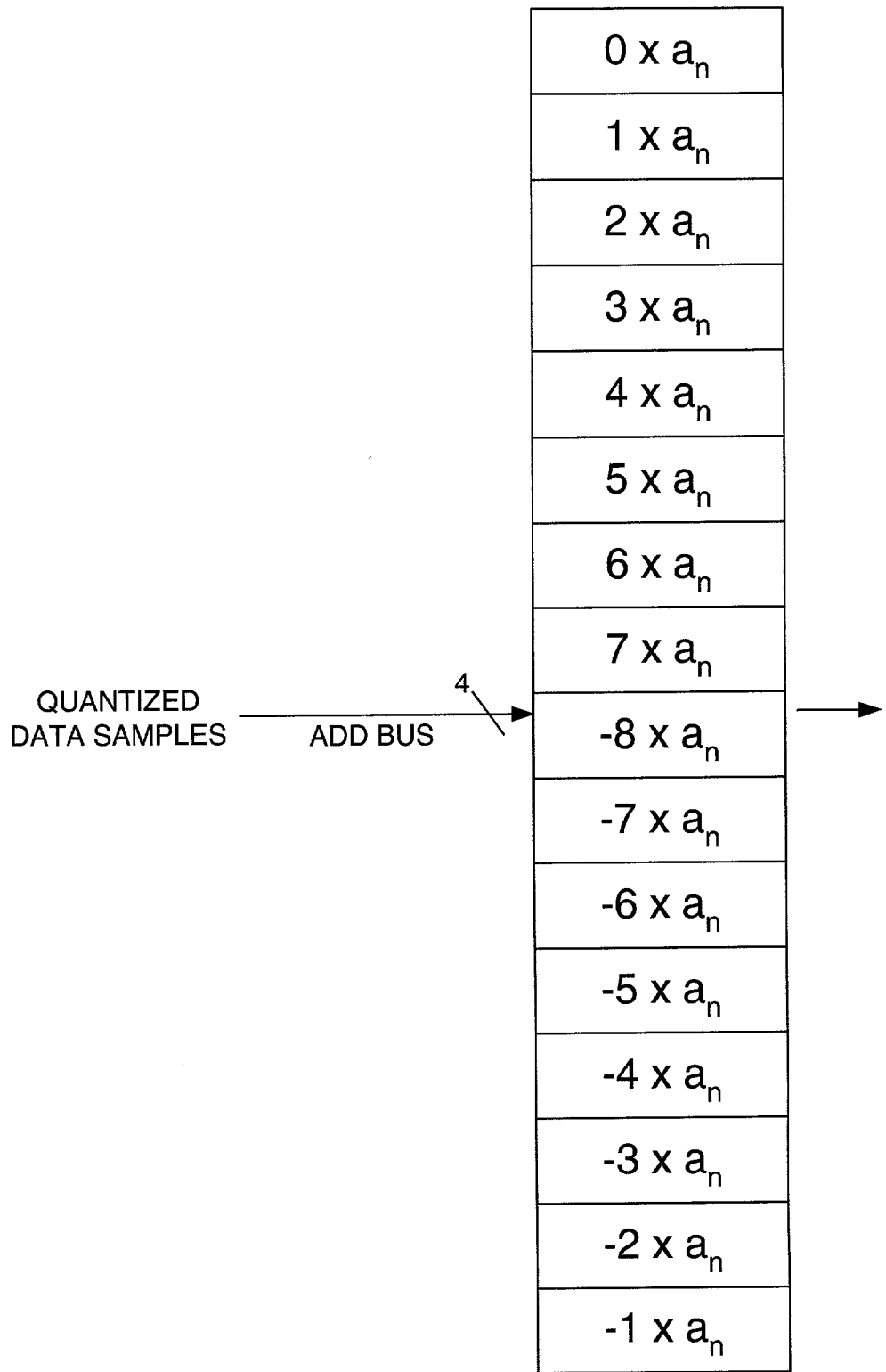


FIG. 14

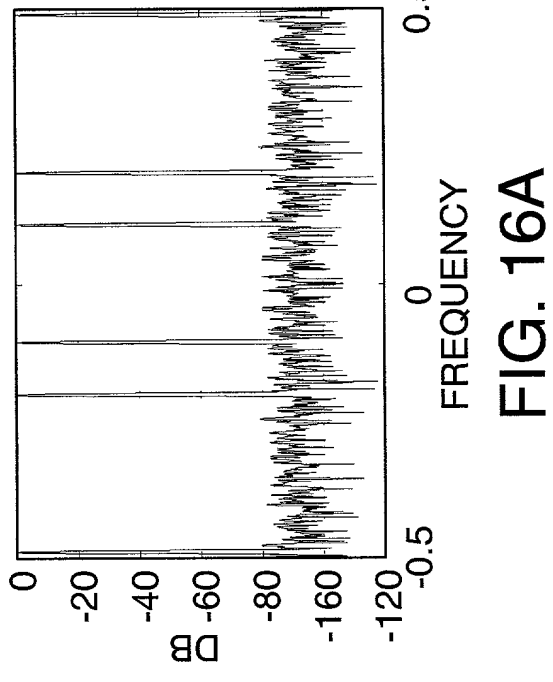


FIG. 16A

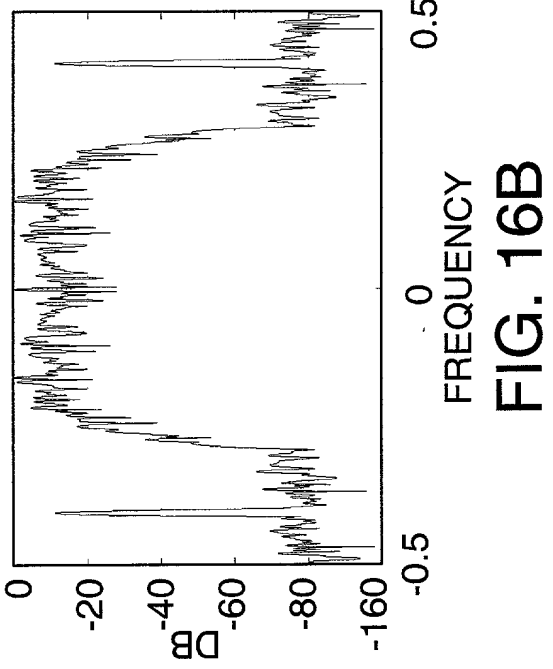


FIG. 16B

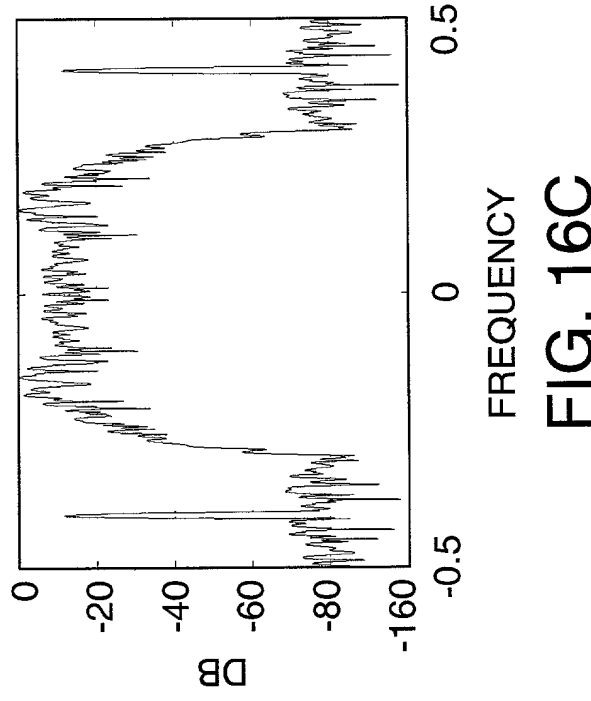


FIG. 16C

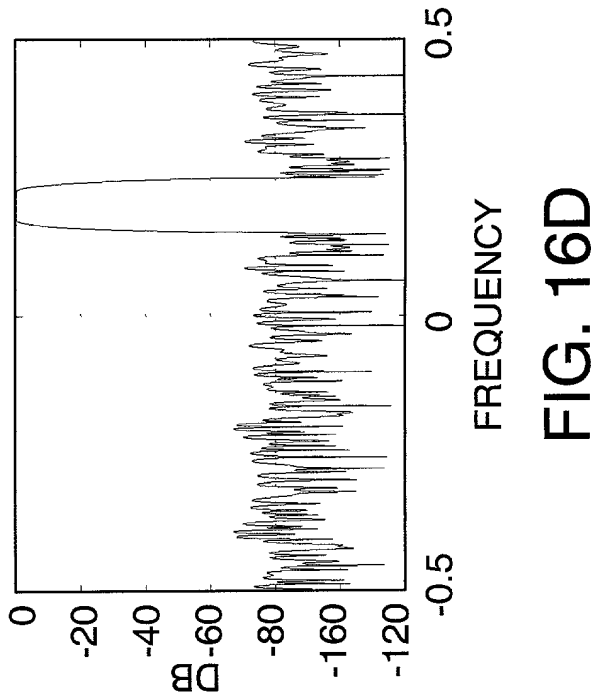
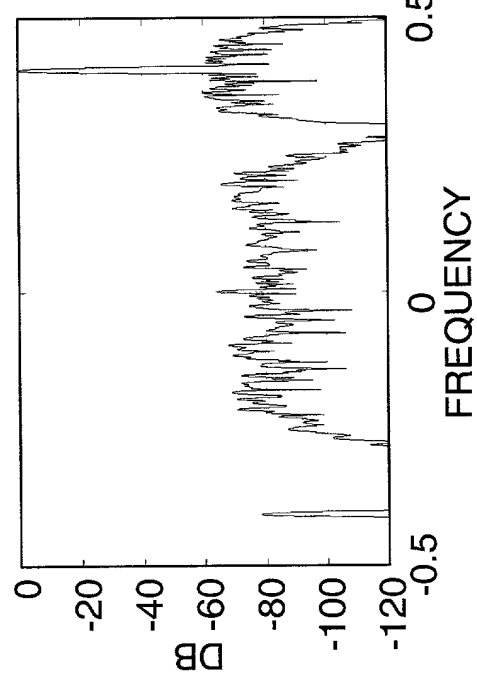
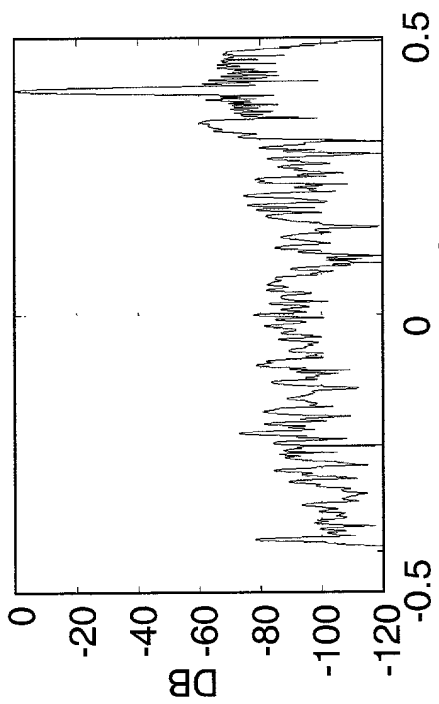


FIG. 16D



**FIG. 16E**



**FIG. 16F**

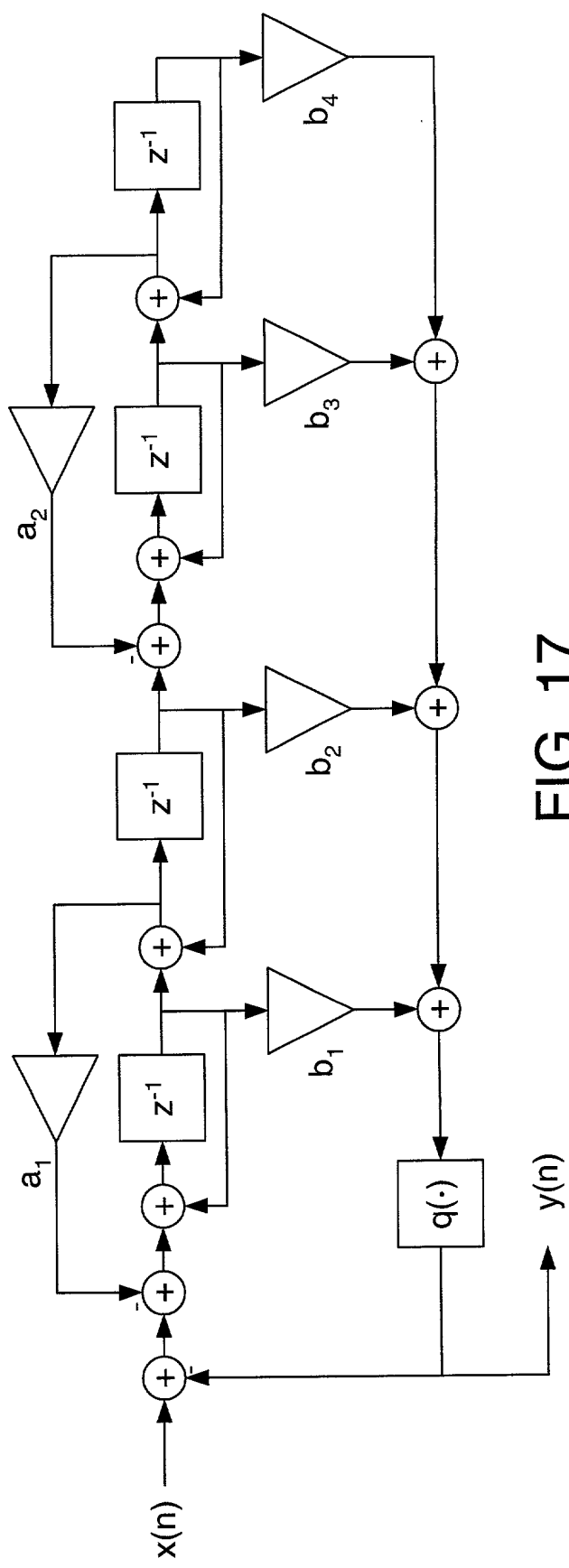


**FIG. 17**

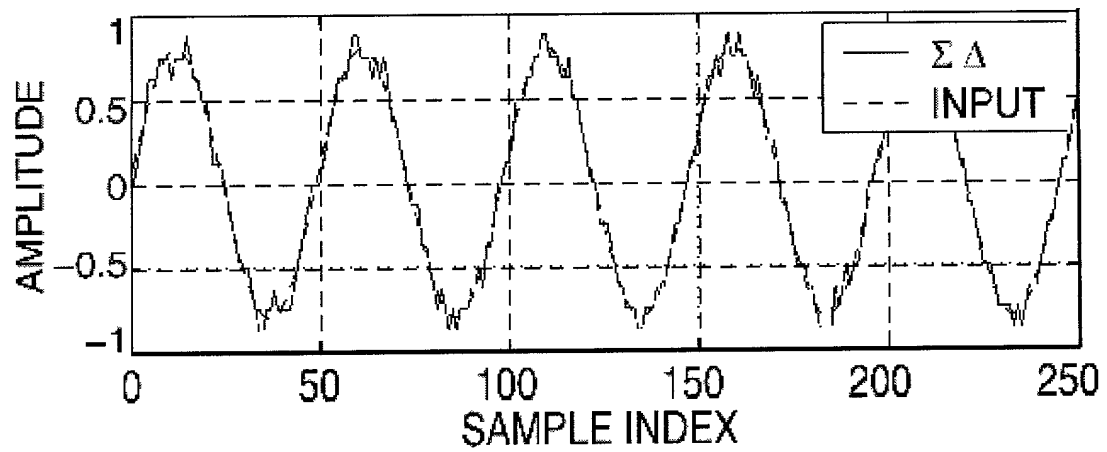


FIG. 18A

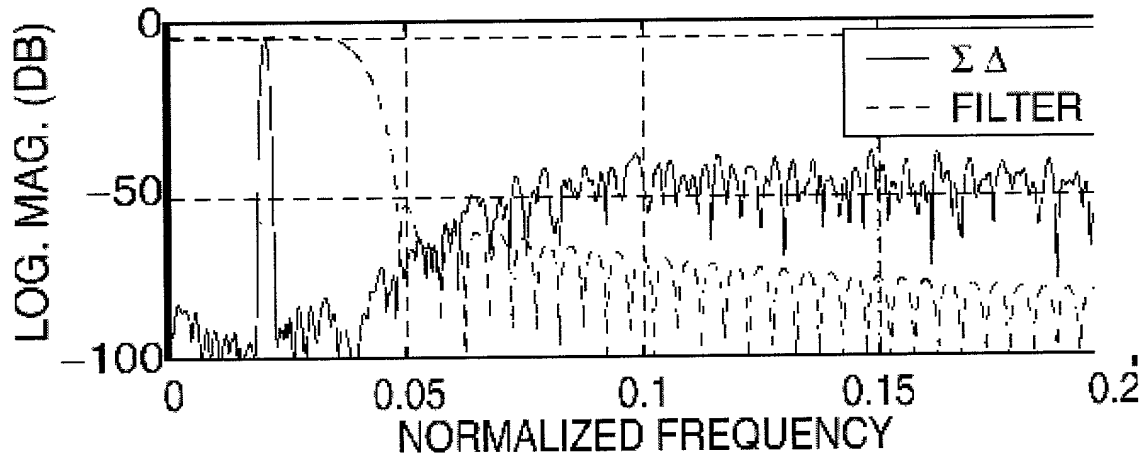


FIG. 18B

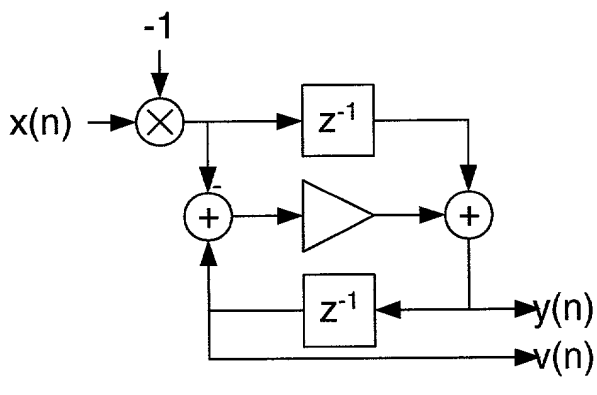


FIG. 19A

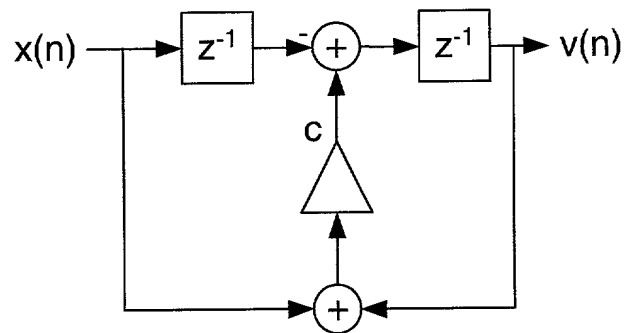


FIG. 19B

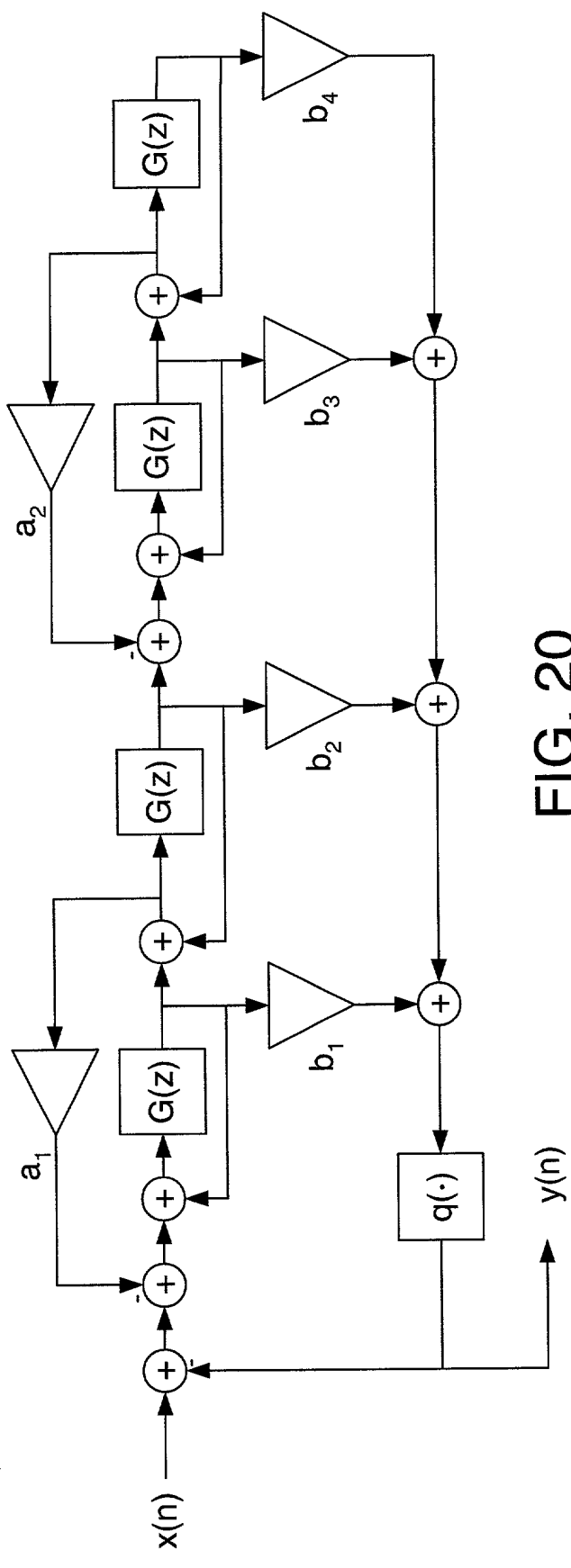


FIG. 20

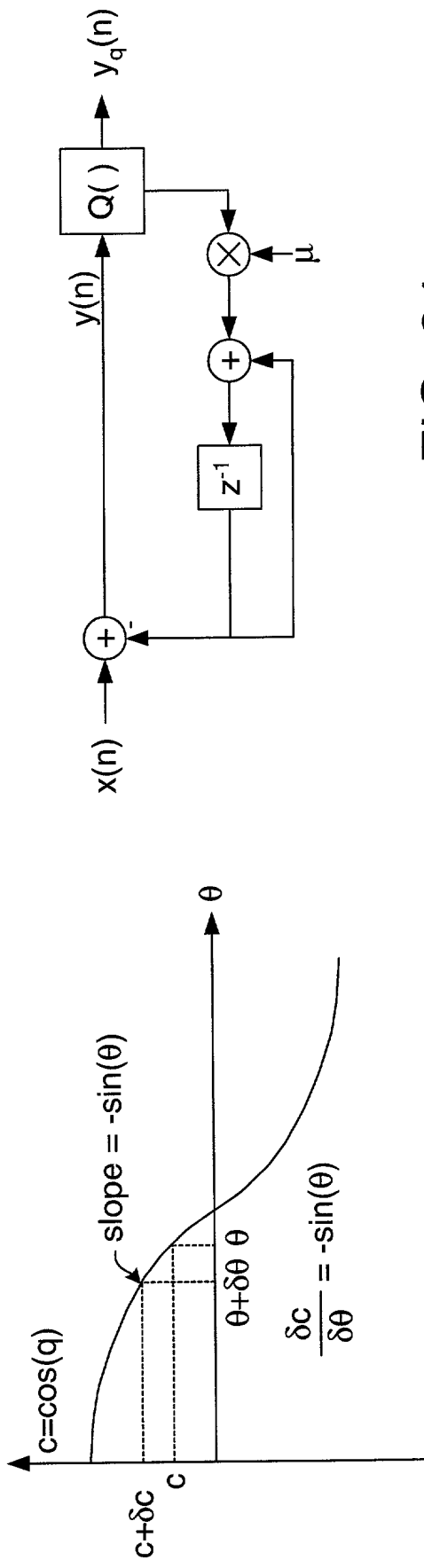


FIG. 24

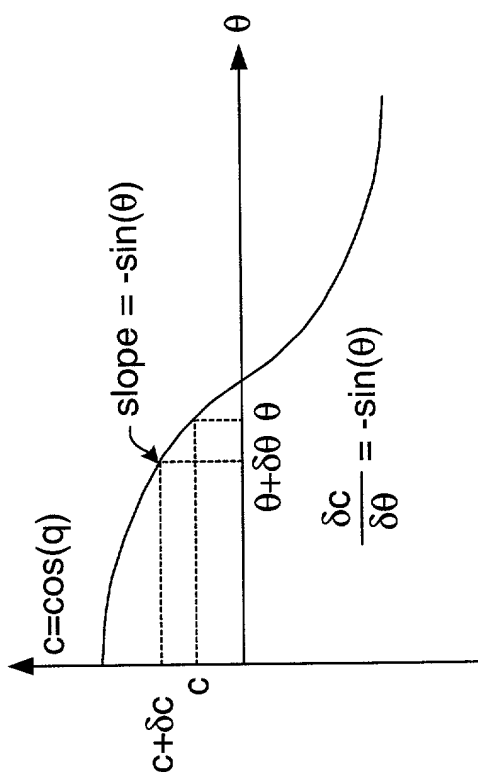
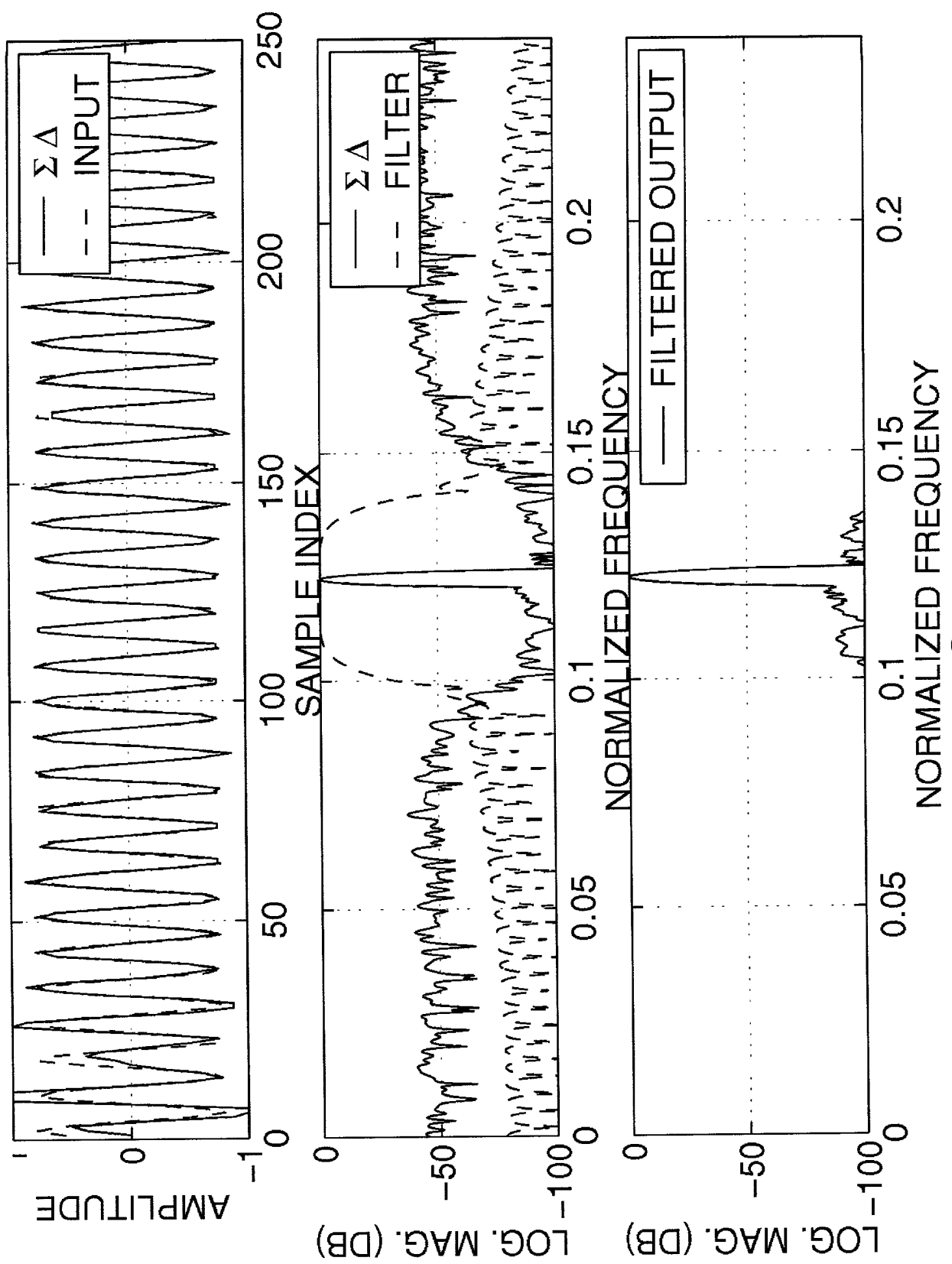
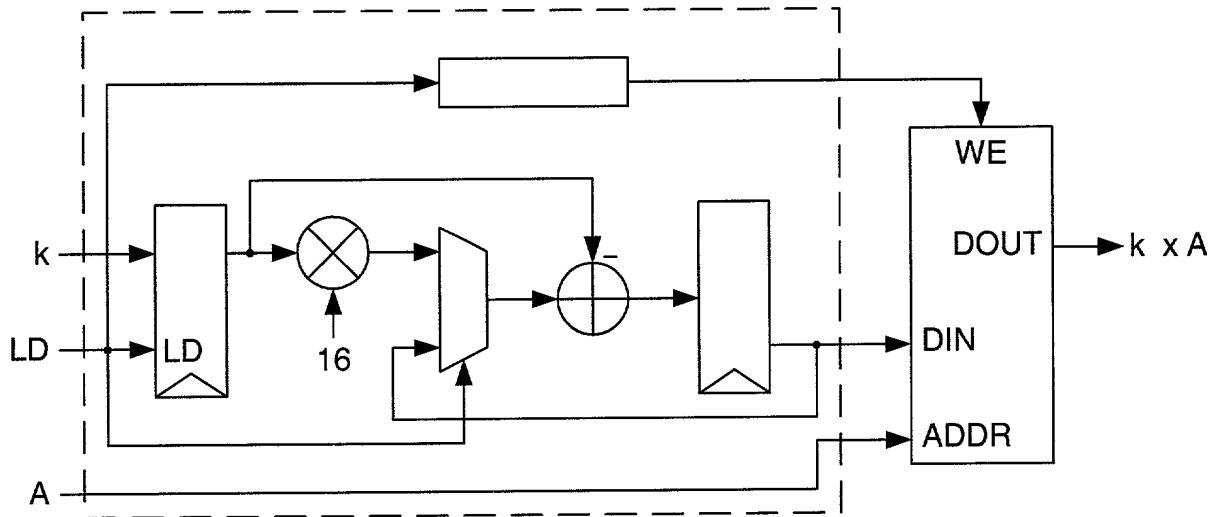


FIG. 22



**FIG. 21**



**FIG. 23**

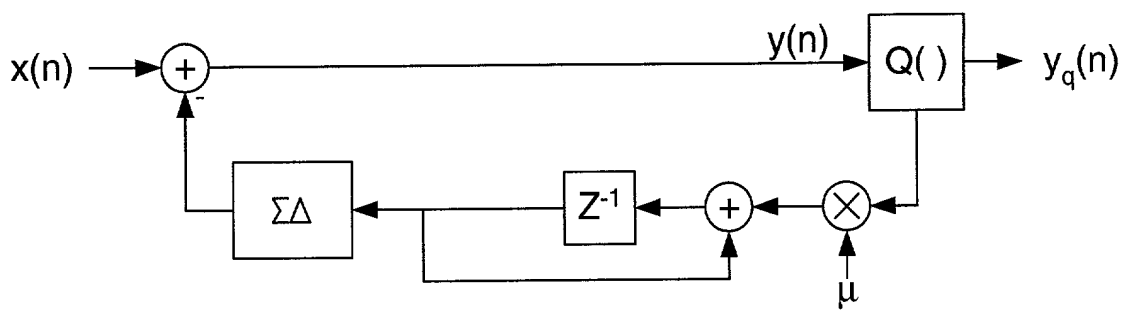


**FIG. 26**

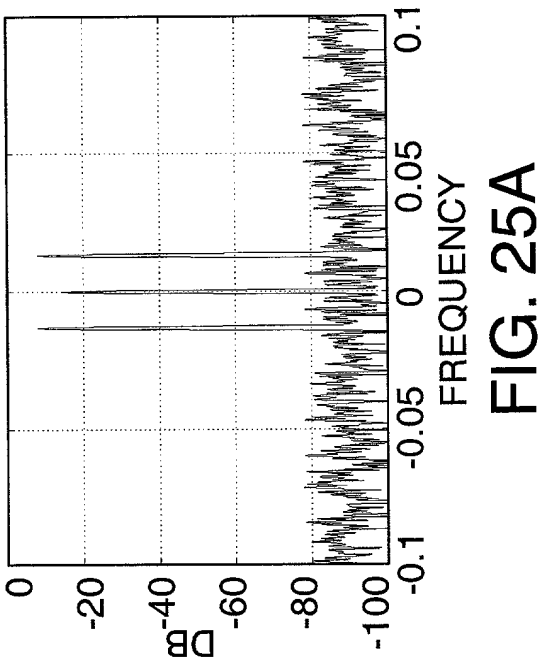


FIG. 25A

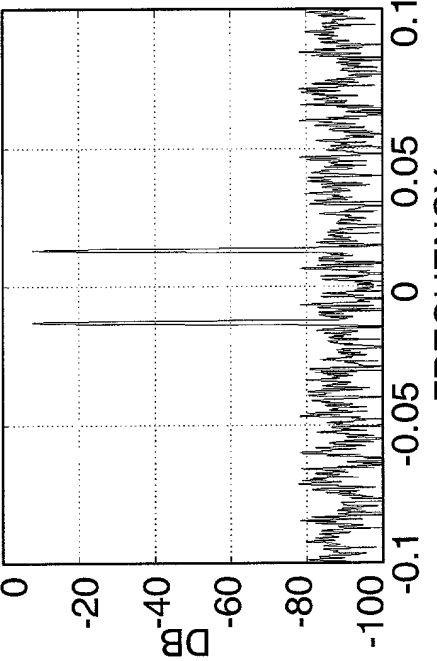


FIG. 25B

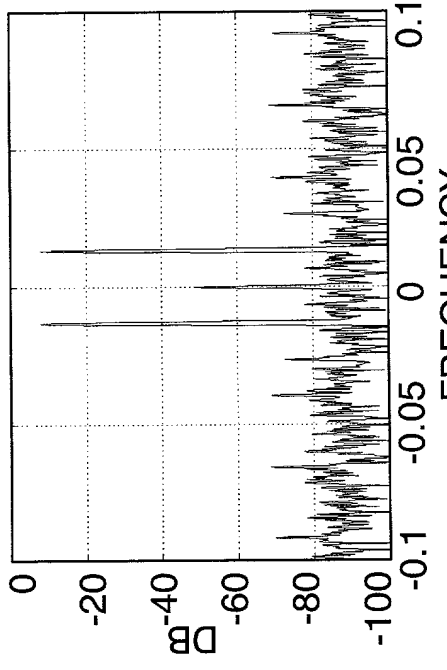


FIG. 25C

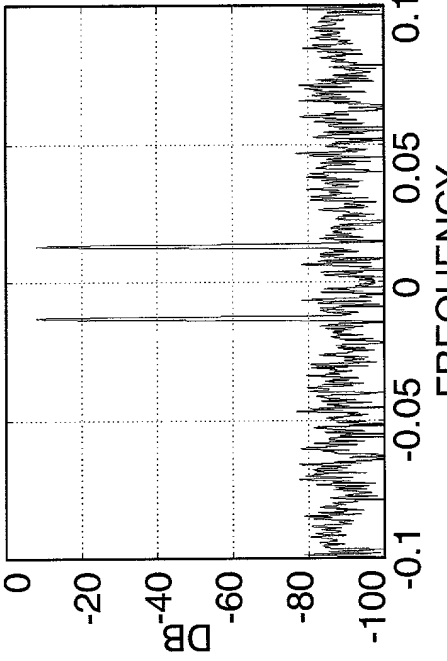
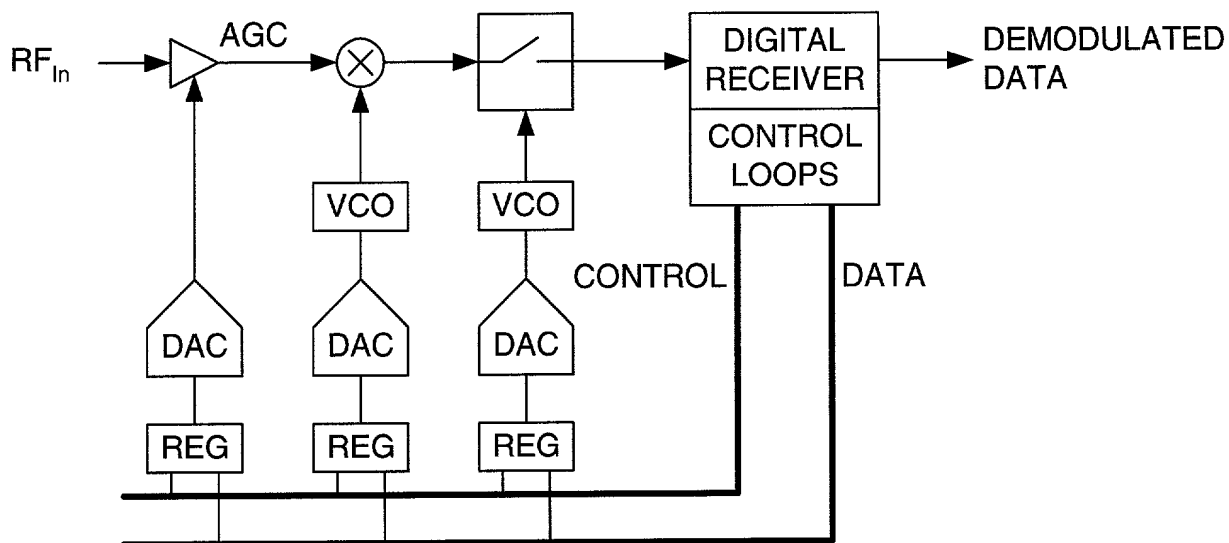
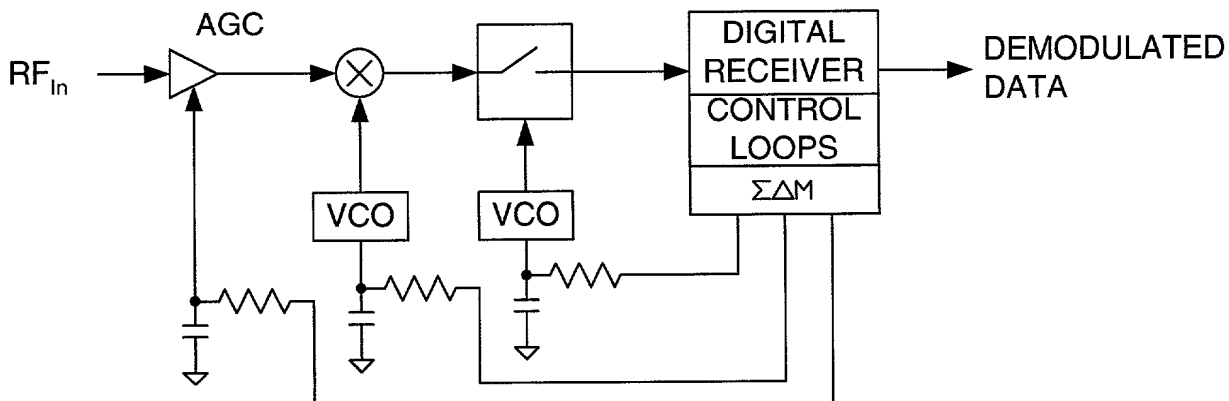


FIG. 25D



**FIG. 27**



**FIG. 28**

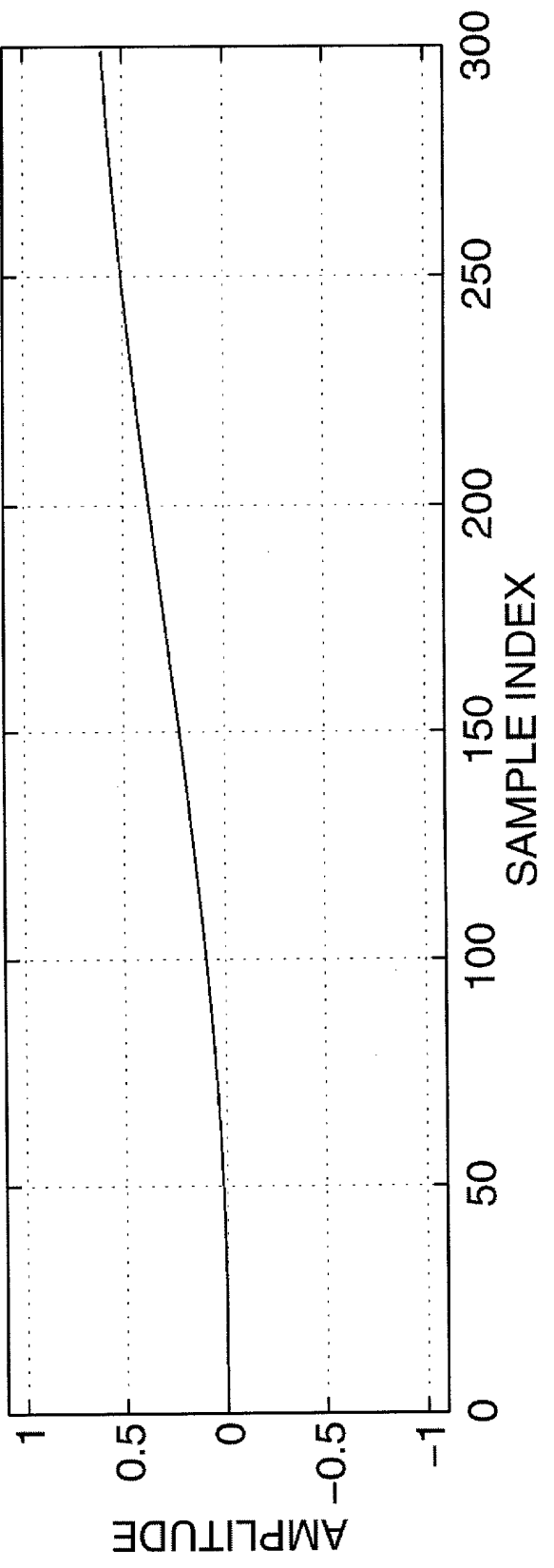
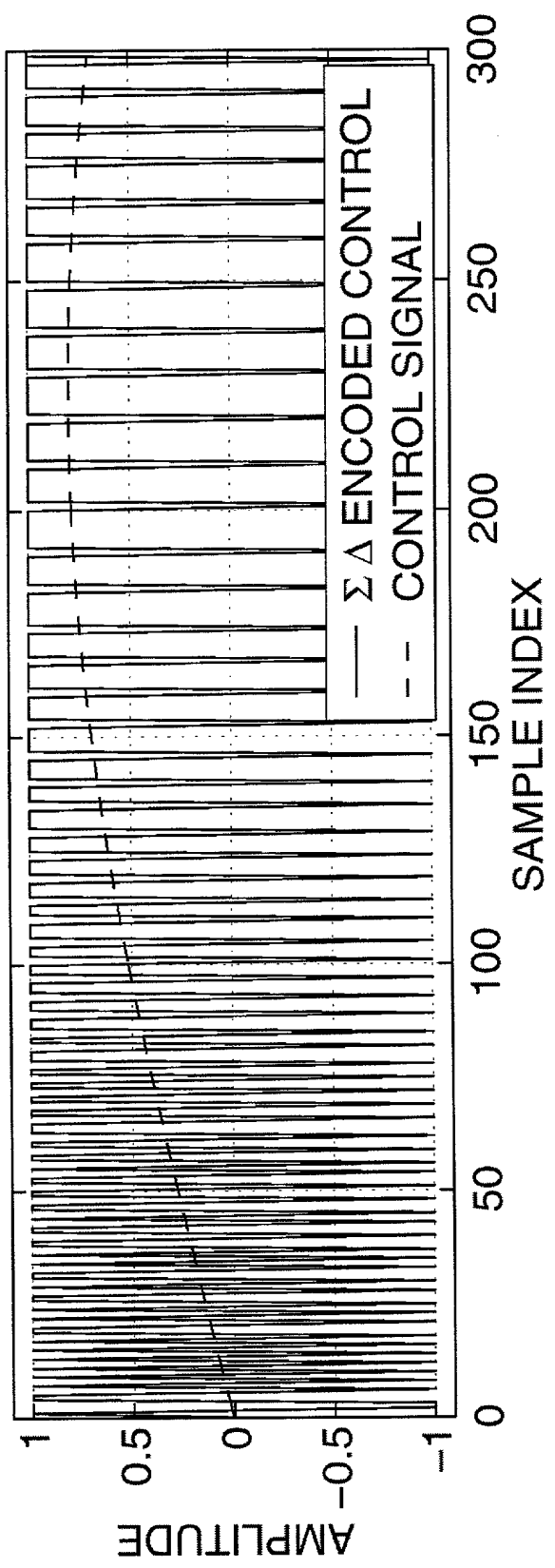


**FIG. 29**

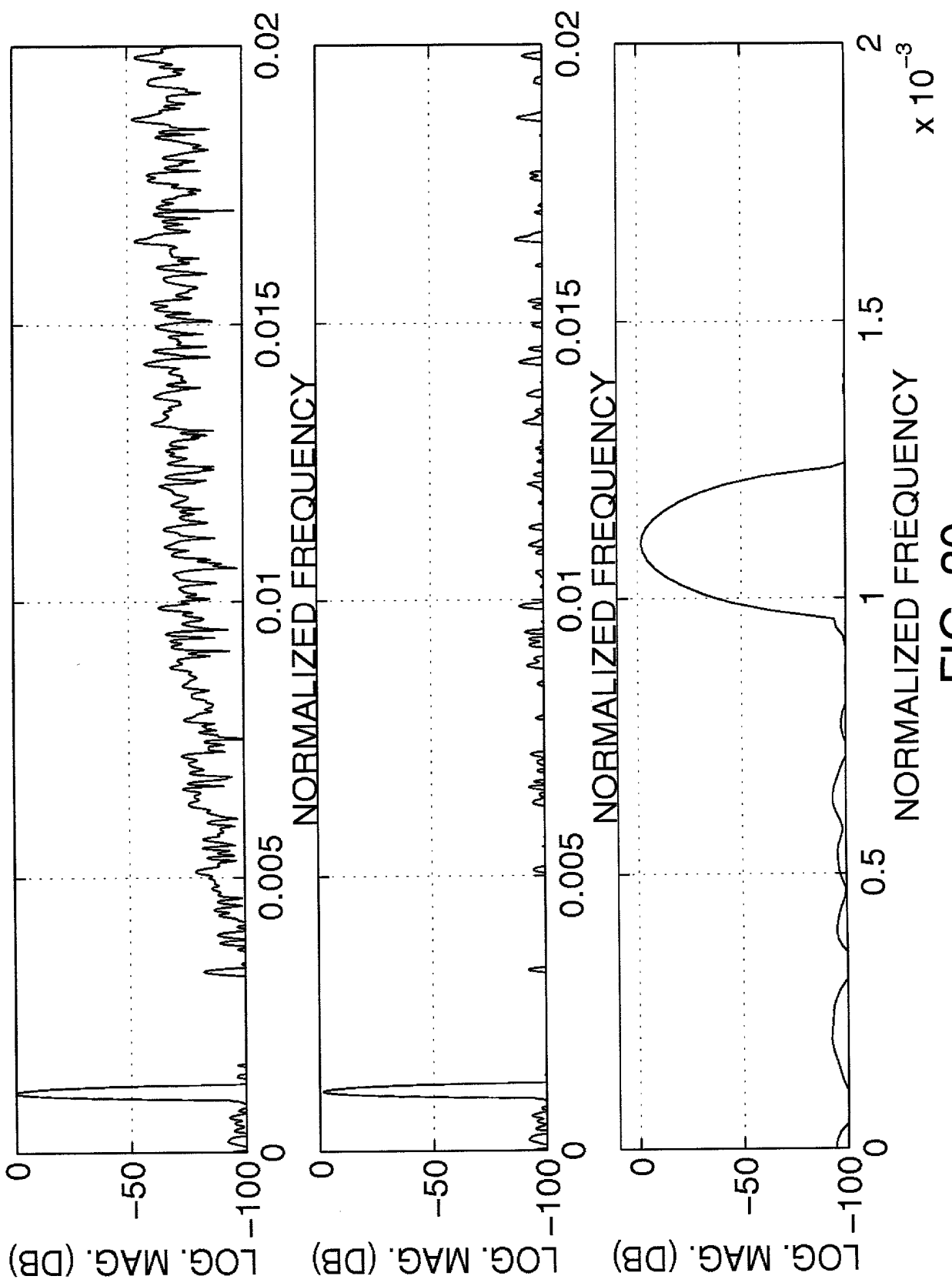


FIG. 30

## DECLARATION FOR PATENT APPLICATION

As a below named inventor, I hereby declare that:

My residence, post office address and citizenship are as stated below adjacent to my name.

I believe I am the original, first and sole inventor (if only one name is listed below) or an original, first and joint inventor (if plural names are listed below) of subject matter (process, machine, manufacture, or composition of matter, or an improvement thereof) that is disclosed and/or claimed and for which a patent is solicited by way of the application entitled

## TUNABLE NARROW-BAND FILTER INCLUDING SIGMA-DELTA MODULATOR

which (check)

- [ X ] is attached hereto.  
[ ] and is amended by the Preliminary Amendment attached hereto.  
[ ] was filed on \_\_\_\_\_ as Application Serial No. \_\_\_\_\_.  
[ ] and was amended on \_\_\_\_\_ (if applicable).

I hereby state that I have reviewed and understand the contents of the above identified application, including the claims, including portions amended by any amendment referred to above.

I acknowledge the duty to disclose information which is material to the examination of this application in accordance with Title 37, Code of Federal Regulations, § 1.56(a).

I hereby claim foreign priority benefits under title 35, United States Code, § 119 of any foreign application(s) for patent or inventor's certificate listed below and have also identified below any foreign application for patent or inventor's certificate having a filing date before that of the application on which priority is claimed:

Prior Foreign Application(s)	Priority Claimed			
(Number)	(Country)	(Day/Month/Year Filed)	Yes	No

I hereby claim the benefit under 35 U.S.C. § 119(e) of any United States provisional application(s) listed below

(Application Number(s))	(Filing Date (MM/DD/YYYY))

I hereby claim the benefit under Title 35, United States Code, § 120 of any United States application(s) listed below and, insofar as any subject matter of this application is not disclosed in the prior United States application in the manner provided by the first paragraph of Title 35, United States Code, § 112, I acknowledge the duty to disclose material information as defined in Title 37, Code of Federal Regulations, § 1.56(a) which occurred between the filing date of the prior application(s) and the national or PCT international filing date of this application:

09/394,123 (Application Serial No.)	September 10, 1999 (Filing Date)	Pending (Status-patented, pending, abandoned)
--	-------------------------------------	--

(Application Serial No.)	(Filing Date)	(Status-patented, pending, abandoned)
--------------------------	---------------	---------------------------------------

I hereby appoint the following attorney(s) and/or agent(s) to prosecute this application and to transact all business in the United States Patent and Trademark Office connected herewith:

Keith A. Chanroo (36,480), Edel M. Young (32,451), and Lois D. Cartier (40,941) all located at Xilinx, Inc., 2100 Logic Drive, San Jose, California 95124, and

Arthur J. Behiel (39,603) located at the Law Office of Arthur Joseph Behiel, 7041 Koll Center Parkway, Suite 280, Pleasanton, California 94566.

Address all telephone calls to: Edel M. Young at Telephone No. (408) 879-4969

Address all correspondence to: Edel M. Young  
Xilinx, Inc.

2100 Logic Drive  
San Jose, California 95124

I hereby declare that all statements made herein of my own knowledge are true and that all statements made on information and belief are believed to be true; and further that these statements were made with the knowledge that willful false statements and the like so made are punishable by fine or imprisonment, or both, under Title 18, United States Code, § 1001 and that such willful false statements may jeopardize the validity of the application or any patent issued thereon.

Full name of sole or first inventor Christopher H. Dick

Inventor's signature \_\_\_\_\_ Date \_\_\_\_\_

Residence 1035 Coleman Road #7120, San Jose, CA 95123 Citizenship Australia

Post Office Address 1035 Coleman Road #7120, San Jose, CA 95123

Full name second inventor Frederic J. Harris

Inventor's signature \_\_\_\_\_ Date \_\_\_\_\_

Residence 2234 Debco Drive, San Diego, CA 92045 Citizenship United States

Post Office Address 2234 Debco Drive, San Diego, CA 92045

Full name third inventor N/A

Inventor's signature \_\_\_\_\_ Date \_\_\_\_\_

Residence \_\_\_\_\_ Citizenship \_\_\_\_\_

Post Office Address \_\_\_\_\_

Full name fourth inventor N/A

Inventor's signature \_\_\_\_\_ Date \_\_\_\_\_

Residence \_\_\_\_\_ Citizenship \_\_\_\_\_

Post Office Address \_\_\_\_\_